Theory of Stationary Electrode Polarography

Single Scan and Cyclic Methods Applied to Reversible, Irreversible, and Kinetic Systems

RICHARD S. NICHOLSON and IRVING SHAIN
Chemistry Department, University of Wisconsin, Madison, Wis.

▶ **The theory of stationary electrode polarography for both single scan and cyclic triangular wave experiments has been extended to systems in which preceding, following, or catalytic (cyclic) chemical reactions are coupled with reversible or irreversible charge transfers. A numerical method was developed for solving the integral equations obtained from the boundary value problems, and extensive data were calculated which permit construction of stationary electrode polarograms from theory. Correlations of kinetic and experimental parameters made it possible to develop diagnostic criteria so that unknown systems can be characterized by studying the variation of peak current, half-peak potential, or ratio of anodic to cathodic peak currents as a function of rate of voltage scan.**

STATIONARY ELECTRODE POLAROGRAPHY (*6*) (voltammetry with linearly varying potential) has found wide application in analysis and in the investigation of electrolysis mechanisms. For analysis, the method is more sensitive and faster than polarography with the dropping mercury electrode (*37*), and when used with stripping analysis, can be extended to trace determinations (*7, 17, 45*). In studying the mechanism of electrode reactions, the use of stationary electrodes with a cyclic potential scan makes it possible to investigate the products of the electrode reaction and detect electroactive intermediates (*10, 11, 18*). Furthermore, the time scale for the method can be varied over an extremely wide range, and both relatively slow and fairly rapid reactions can be studied with a single technique. Various electrodes have been used in these studies, but the most important applications have involved the hanging mercury drop electrode [reviewed by Kemula (*16*) and Riha (*36*)], and the dropping mercury electrode [reviewed by Vogel (*50*)].

Since the first application of the method by Matheson and Nichols (*21*), numerous investigators have contributed to the theory of stationary electrode polarography. The first were Randles (*29*) and Sevcik (*44*) who considered the single scan method for a reversible reaction taking place at a plane electrode. The theory was extended to totally irreversible charge transfer reactions by Delahay (*4*), and later, Matsuda and Ayabe (*23*) rederived the Randles-Sevcik reversible theory, the Delahay irreversible theory, and then extended the treatment to the intermediate quasi-reversible case. Other workers also have considered both reversible (*13, 22, 32, 35*) and totally irreversible (*12, 32*) reactions taking place at plane electrodes.

In addition, the theory of the single scan method has been extended to reversible reactions taking place at cylindrical electrodes (*25*) and at spherical electrodes (*9, 31, 32, 35*). Totally irreversible reactions taking place at spherical electrodes (*8, 32*) also have been discussed. Further contributions to the theory have included systems in which the products of the electrode reaction are deposited on an inert electrode (*2*); the reverse reaction, involving the dissolution of a deposited film (*26*); and systems involving multi-electron consecutive reactions, where the individual steps take place at different potentials (*14, 15*).

Even in the cases involving reversible reactions at plane electrodes, the theoretical treatment is relatively difficult, ultimately requiring some sort of numerical analysis. Because of this, the more complicated cases in which homogeneous chemical reactions are coupled to the charge transfer reaction have received little attention. Saveant and Vianello developed the theory for the catalytic mechanism (*39*), the preceding chemical reaction (*38, 41*), and also have discussed the case involving a very rapid reaction following the charge transfer (*40*). Reinmuth (*32*) briefly discussed the theory for a system in which a first order chemical reaction follows the charge transfer.

The mathematical complexity also has prevented extensive study of the cyclic triangular wave methods, in spite of the value of this approach. Sevcik (*44*) qualitatively discussed the method for reversible reactions at a plane electrode under steady state conditions—i.e., after many cycles when no further changes in the concentration distributions take place in the solution from one cycle to the next. Later Matsuda (*22*) presented the complete theory for this multisweep cyclic triangular wave method, for a reversible reaction at a plane electrode. The only other contributions to the theory of cyclic methods were those of Gokhshtein (*13*) (reversible reactions), Koutecky (*19*) (reversible and quasi-reversible reactions), and Weber (*51*) (catalytic reactions). A generalized function of time was included in each of these derivations, which thus could be extended to cyclic triangular-wave voltammetry. In the last two papers, however, the case actually considered was for a cyclic step-functional potential variation.

Because of the increased interest in stationary electrode polarography, it has become important to extend the theory to include additional kinetic cases. Furthermore, many of the recent applications of cyclic triangular wave voltammetry have involved only the first few cycles, rather than the steady state multisweep experiments. Therefore, a general approach was sought, which could be applied to all these cases. In considering the mathematical approaches of other authors, at least three have been used previously: applications of Laplace transform techniques, direct numerical solution using finite difference techniques, and conversion of the boundary value problem to an integral equation.

The first approach is the most elegant, but is applicable only to the simplest case of a reversible charge transfer reaction (*2, 19, 31, 35, 44*), and also to the catalytic reaction (*51*). Even in these cases, definite integrals arise which can only be evaluated numerically.

The second approach (*8, 9, 25, 29*) is the least useful of the three, because functional relations which may exist between the experimental parameters are usually embodied in extensive

numerical tabulations and are often missed. Thus, the results may depend on an extremely large number of variables. This is particularly so in the more complicated cases involving coupled chemical reactions, which may require the direct simultaneous solution of three partial differential equations together with three initial and six boundary conditions.

The third method possesses the advantages of the first, and yet is more generally applicable. Several methods can be used to convert the boundary value problem to an integral equation (*33*), and at least two methods of solving the resulting integral equations have been used. The series solution proposed by Reinmuth (*32*) is very straightforward, but only in cases involving totally irreversible charge transfer does it provide a series which is properly convergent over the entire potential range. [This approach to obtaining series solutions is essentially the same as used by Smutek (*47*) for irreversible polarographic waves. Series solutions of the same form can also be obtained directly from the differential equations, as was shown recently by Buck (*3*)]. Reinmuth has outlined a method for evaluating these series in regions where they are divergent (*33*), but attempts to use that approach in this laboratory (with a Bendix Model G-15 digital computer) produced erratic results.

The methods most frequently used for solving the integral equations have been numerical (*4*, *12*, *13*, *22*, *23*, *26*, *39*) and an adaptation of the approach suggested by Gokhshtein (*13*) was used in this work. The method which was developed is generally applicable to all of the cases mentioned above, all additional first order kinetic cases of interest, and both single scan and cyclic triangular wave experiments. Except for reversible, irreversible, and catalytic reactions, the treatment is limited to plane electrodes because of the marked increase in complexity of the theory for most of the kinetic cases if an attempt is made to account for spherical diffusion rigorously. Conditions under which derivations for plane electrodes can be used for other geometries have been discussed by Berzins and Delahay (*2*). An empirical approach to making approximate corrections for the spherical contribution to the current will be described elsewhere. The cases considered here all involve reductions for the first charge transfer step, but extension to oxidations is obvious.

To present a logical discussion, each of the kinetic cases was compared to the corresponding reversible or irreversible reaction which would take place without the kinetic complication. Thus, it was necessary to include in this work a substantial discussion of these two cases, in spite of the extensive previous work. However, this makes it possible to discuss the numerical method proposed here in terms of the simplest possible case for clarity, and at the same time summarizes the widely scattered previous work in a form which is most convenient for comparison of experimental results with theory.

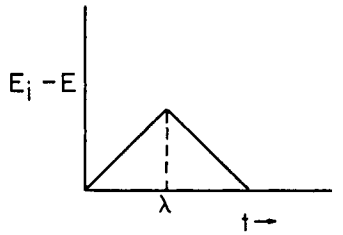

Figure 1. Wave form for cyclic triangular wave voltammetry

I. REVERSIBLE CHARGE TRANSFER

Boundary Value Problem. For a reversible reduction of an oxidized species O to a reduced species R,

$$O + ne \rightleftharpoons R \qquad \text{(I)}$$

taking place at a plane electrode, the boundary value problem for stationary electrode polarography is

$$\frac{\partial C_O}{\partial t} = D_O \frac{\partial^2 C_O}{\partial x^2} \qquad (1)$$

$$\frac{\partial C_R}{\partial t} = D_R \frac{\partial^2 C_R}{\partial x^2} \qquad (2)$$

$t = 0, x \geqslant 0$:

$$C_O = C_O^*;\ C_R = C_R^*\ (\sim 0) \qquad (3)$$

$t \geqslant 0, x \rightarrow \infty$: $C_O \rightarrow C_O^*;\ C_R \rightarrow 0$ (4)

$t > 0, x = 0$:

$$D_O\left(\frac{\partial C_O}{\partial x}\right) = -D_R\left(\frac{\partial C_R}{\partial x}\right) \qquad (5a)$$

$$C_O/C_R = \exp[(nF/RT)(E - E^\circ)] \qquad (5b)$$

where C_O and C_R are the concentrations of substances O and R, x is the distance from the electrode, t is the time, C_O^* and C_R^* are the bulk concentrations of substances O and R, D_O and D_R are the diffusion coefficients, n is the number of electrons, E is the potential of the electrode, E° is the formal electrode potential, and R, T, and F have their usual significance. The applicability of the Fick diffusion equations and the initial and boundary conditions has been discussed by Reinmuth (*33*).

For the case of stationary electrode polarography, the potential in Equation 5b is a function of time, given by the relations

$$0 < t \leqslant \lambda \quad E = E_i - vt \qquad (6a)$$

$$\lambda \leqslant t: \quad E = E_i - 2v\lambda + vt \qquad (6b)$$

where E_i is the initial potential, v is the rate of potential scan, and λ is the time at which the scan is reversed (Figure 1).

Equations 6a and 6b can be substituted into Equation 5b to obtain the boundary condition in an abridged form:

$$C_O/C_R = \theta S_\lambda(t) \qquad (7)$$

where

$$\theta = \exp[(nF/RT)(E_i - E^\circ)] \qquad (8)$$

$$S_\lambda(t) = \begin{cases} e^{-at} \text{ for } t \leqslant \lambda \\ e^{at - 2a\lambda} \text{ for } t \geqslant \lambda \end{cases} \qquad (9)$$

and

$$a = nFv/RT \qquad (10)$$

If t is always less than λ, then Equation 7 reduces to

$$C_O/C_R = \theta e^{-at} \qquad (11)$$

which is the same boundary condition that has been used previously for theoretical studies of the single scan method for a reversible charge transfer.

The direct use of the Laplace transform to solve this boundary value problem is precluded by the form of Equation 7. However, the differential equations can be converted into integral equations by taking the Laplace transform of Equations 1 to 4, solving for the transform of the surface concentrations in terms of the transform of the surface fluxes, and then applying the convolution theorem (*33*):

$$C_O(0,t) = C_O^* - \frac{1}{\sqrt{\pi D_O}} \int_0^t \frac{f(\tau)d\tau}{\sqrt{t - \tau}} \qquad (12)$$

$$C_R(0,t) = \frac{1}{\sqrt{\pi D_R}} \int_0^t \frac{f(\tau)d\tau}{\sqrt{t - \tau}} \qquad (13)$$

where

$$f(t) = D_0\left(\frac{\partial C_O}{\partial x}\right)_{x=0} = i/nFA \qquad (14)$$

The boundary condition of Equation 7 now can be combined with Equations 12 and 13, to eliminate the concentration terms and obtain a single integral equation, which has as its solution the flux of substance O at the electrode surface:

$$\int_0^t \frac{f(\tau)d\tau}{\sqrt{t - \tau}} = \frac{C_O^* \sqrt{\pi D_O}}{1 + \gamma\theta S_\lambda(t)} \qquad (15)$$

where

$$\gamma = \sqrt{D_O/D_R} \qquad (16)$$

Referring to Equation 10, it can be noted that the term at is dimensionless

$$at = nFvt/RT = (nF/RT)(E_i - E) \qquad (17)$$

and is proportional to the potential. Since the ultimate goal is to calculate current-potential curves rather than

Table I. Current Functions $\sqrt{\pi}\chi(at)$ for Reversible Charge Transfer (Case I)

$(E - E_{1/2})n$ mv.	$\sqrt{\pi}\chi(at)$	$\phi(at)$	$(E - E_{1/2})n$ mv.	$\sqrt{\pi}\chi(at)$	$\phi(at)$
120	0.009	0.008	− 5	0.400	0.548
100	0.020	0.019	10	0.418	0.596
80	0.042	0.041	15	0.432	0.641
60	0.084	0.087	20	0.441	0.685
50	0.117	0.124	25	0.445	0.725
45	0.138	0.146	−28.50	0.4463	0.7516
40	0.160	0.173	30	0.446	0.763
35	0.185	0.208	35	0.443	0.796
30	0.211	0.236	40	0.438	0.826
25	0.240	0.273	50	0.421	0.875
20	0.269	0.314	−60	0.399	0.912
15	0.298	0.357	80	0.353	0.957
10	0.328	0.403	100	0.312	0.980
5	0.355	0.451	120	0.280	0.991
0	0.380	0.499	150	0.245	0.997

To calculate the current:

(1) $i = i$(plane) + i(spherical correction).
(2) $= nFA\sqrt{aD_O}C_O^*\sqrt{\pi}\chi(at) + nFAD_OC_O^*(1/r_o)\phi(at)$
(3) $= 602\, n^{3/2}A\sqrt{D_O v}\, C_O^*[\sqrt{\pi}\chi(at) + 0.160(\sqrt{D_O}/r_o\sqrt{nv})\phi(at)]$, amperes.

Units for (3) are: A, sq. cm.; D_O, sq. cm./sec.; v, volt/sec.; C_O^*, moles/liter; r_o, cm.

current-time curves, it is useful to make all calculations with respect to at rather than t. This can be accomplished by a change in variable

$$\tau = z/a \tag{18}$$

$$f(t) = g(at) \tag{19}$$

and Equation 15 becomes

$$\int_0^{at} \frac{g(z)dz}{\sqrt{a}\sqrt{at - z}} = \frac{C_O^*\sqrt{\pi D_O}}{1 + \gamma\theta S_{a\lambda}(at)} \tag{20}$$

This integral equation can be made dimensionless (especially important if numerical methods are used) by the substitution

$$g(at) = C_O^*\sqrt{\pi D_O a}\,\chi(at) \tag{21}$$

and the final form of the integral equation is:

$$\int_0^{at} \frac{\chi(z)dz}{\sqrt{at - z}} = \frac{1}{1 + \gamma\theta S_{a\lambda}(at)} \tag{22}$$

The solution to Equation 22 provides values of $\chi(at)$ as a function of at, for a given value of $\gamma\theta$. From Equations 5b and 7, the values of at are related to the potential by

$$E = E^\circ - (RT/nF)\ln\gamma + (RT/nF)[\ln\gamma\theta + \ln S_{a\lambda}(at)] \tag{23a}$$

or

$$(E - E_{1/2})n = (RT/F)[\ln\gamma\theta + \ln S_{a\lambda}(at)] \tag{23b}$$

where $E_{1/2}$ is the polarographic half wave potential

$$E_{1/2} = E^\circ + (RT/nF)\ln\sqrt{D_R/D_O} \tag{24}$$

Thus, values of $\chi(at)$ can be regarded as values of $\chi[(E - E_{1/2})n]$, and will ultimately furnish values of the current as a function of potential (Equations 14, 19, 21):

$$i = nFAC_O^*\sqrt{\pi D_O a}\,\chi(at) \tag{25}$$

The values of $\chi(at)$ are independent of the actual value of $\gamma\theta$ selected, provided ln $\gamma\theta$ is larger than perhaps 6, and a formal proof has been given by Reinmuth (*35*). This corresponds to the usual experimental procedure of selecting an initial potential anodic of the foot of the wave, and in effect reduces the number of variables involved by one.

Numerical Solution. Although Equation 22 has been solved in several ways, only the numerical approaches appeared to be readily applicable to the cyclic experiment. The technique developed here involves dividing the range of integration from $at = 0$ to $at = M$ into N equally spaced subintervals by a change of variable,

$$z = \delta\nu \tag{26}$$

and the definition

$$n = at/\delta \tag{27}$$

Here, δ is the length of the subinterval ($\delta = M/N$), and n is a serial number of the subinterval. Thus, Equation 23 becomes

$$\sqrt{\delta}\int_0^n \frac{\chi(\delta\nu)\,d\nu}{\sqrt{n - \nu}} = \frac{1}{1 + \gamma\theta S_{\delta\lambda}(\delta n)} \tag{28}$$

where n varies from 0 to M in N integral steps. The point of singularity ($n = \nu$) in the kernel in Equation 28 can be removed through an integration by parts to obtain

$$\int_0^n \frac{\chi(\delta\nu)d\nu}{\sqrt{n - \nu}} = 2\left[\chi(0)\sqrt{n} + \int_0^n \sqrt{n - \nu}\, d[\chi(\delta\nu)]\right] \tag{29}$$

The integral on the right hand side of Equation 29 is a Riemann-Stieltjes integral, which can be replaced by its corresponding finite sum (*1*). Eliminating the special points $i = 0$ and $i = n$ from the summation, one obtains

$$\int_0^n \frac{\chi(\delta\nu)d\nu}{\sqrt{n - \nu}} = 2\left[\chi(1)\sqrt{n} + \sum_{i=1}^{n-1}\sqrt{n - i}\,[\chi(i + 1) - \chi(i)]\right] \tag{30}$$

and substituting this result in Equation 28,

$$2\sqrt{\delta}\left[\chi(1)\sqrt{n} + \sum_{i=1}^{n-1}\sqrt{n - i}[\chi(i + 1) - \chi(i)]\right] = \frac{1}{1 + \gamma\theta S_{\delta\lambda}(\delta n)} \tag{31}$$

Equation 31 defines N algebraic equations in the unknown function $\chi(n)$, where each nth equation involves the previous $n - 1$ unknowns. These equations are then solved successively for the values of $\chi(at)$—i.e., $\chi(\delta n)$. When $\delta n \leqslant \delta\lambda$, the function $S_{\delta\lambda}(\delta n)$ is $\exp(-\delta n)$, and when the point in the calculations is reached where $\delta n > \delta\lambda$, the function is replaced by exp $(\delta n - 2\delta\lambda)$. In this way, single scan or cyclic current-potential curves can be calculated easily, and the extension to multicycles is obvious.

Analytical Solution. It is also possible to obtain an analytical solution to Equation 22. It is an Abel integral equation (*48*), and the solution can be written directly as

$$\chi(at) = \frac{L(0)}{\pi\sqrt{at}} + \frac{1}{\pi}\int_0^{at}\frac{1}{\sqrt{at - z}}\left[\frac{dL(at)}{d(at)}\right]_{at=z} dz \tag{32}$$

where $L(at)$ represents the right hand side of Equation 22. Performing the differentiation indicated (using Equation 11 as the boundary condition) the exact solution is

$$\chi(at) = \frac{1}{\pi\sqrt{at}(1 + \gamma\theta)} + \frac{1}{4\pi}\int_0^{at}\frac{dz}{\sqrt{at - z}\cosh^2\left(\frac{\ln\gamma\theta - z}{2}\right)} \tag{33}$$

Equation 33 has been given previously by Matsuda and Ayabe (*23*), and by

Gokhshtein (*13*). If it is assumed that $\gamma\theta$ is large, Equation 33 reduces to the result obtained by Sevcik (*44*) and by Reinmuth (*35*), but such an assumption is not required in this case. Although the definite integral in Equation 33 cannot be evaluated in closed form, several numerical methods (such as the Euler-Maclaurin summation formula or Simpson's rule) can be used, provided the singularity at $at = z$ is first removed by a change of variable (*23*) or an integration by parts (*35*).

Series Solution. If only the single scan method is considered, Equation 22 can be solved in series form, and although the resulting series does not properly converge for all potentials, the form of the results obtained is very useful for comparison of the limiting cases obtained in the kinetic systems.

One possible approach is to expand the right hand side of Equation 22 as an exponential power series in at, as done by Sevcik (*44*), but this cannot be done for most cases involving coupled chemical reactions. Thus, Reinmuth's approach (*32*, *33*) is more general, and the final result is

$$\chi(at) = \frac{1}{\sqrt{\pi}} \sum_{j=1}^{\infty} (-1)^{j+1} \sqrt{j} \times \exp[(-jnF/RT)(E - E_{1/2})] \quad (34)$$

Single Scan Method. In every case, the solution of Equation 22 ultimately requires numerical evaluation which in the past has been carried out with varying accuracy. This has led to some uncertainty in the literature regarding the location of the peak potential with respect to $E_{1/2}$, the height of the peak, the significance of the half-peak potential, etc. For this reason, the calculations were carried out (using the numerical solution, Equation 31) on an IBM 704 digital computer to obtain accurate values of $\chi(at)$ as a function of potential (Table I). Since the hanging mercury drop electrode is frequently used in analytical work, there is also listed a function based on Reinmuth's equation (*35*), from which currents at a spherical electrode can be calculated. The calculations were made using a value of $\delta = 0.01$, with $\ln \gamma\theta = 6.5$, and are accurate to ± 0.001. The temperature was assumed to be 25° C., and values for some other temperature can be obtained by multiplying the potential by the factor $(273.16 + T)/298.16$ (see Equation 23). The factor $\sqrt{\pi}$ was included in the tabulation for convenience in making comparisons with previous work.

The reversible stationary electrode polarogram for a plane electrode exhibits a maximum value of $i_p/(nFA\sqrt{Doa}\ Co^*) = 0.4463$ at a potential

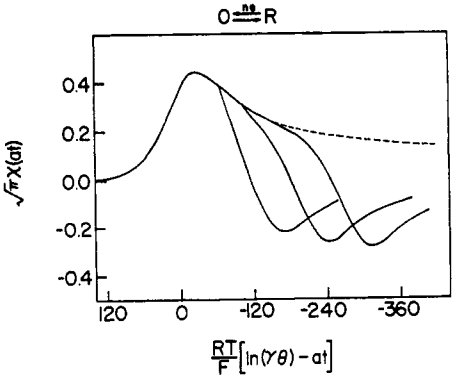

Figure 2. Cyclic stationary electrode polarograms (Case I)

Switching potentials correspond to $(E_{1/2} - E_\lambda)n$ of 64, 105, and 141 mv. for anodic scans

$28.50/n$ millivolts cathodic of $E_{1/2}$,—i.e.,

$$(E_p - E^\circ)n + (RT/F) \ln \gamma = -28.50 \pm 0.05 \text{ mv.} \quad (35)$$

or

$$E_p = E_{1/2} - (1.109 \pm 0.002)(RT/nF) \quad (36)$$

Actually, the peak of a reversible stationary electrode polarogram is fairly broad, extending over a range of several millivolts if values of $\chi(at)$ are determined to about 1%. Thus, it is sometimes convenient to use the half-peak potential as a reference point (*24*), although this has no direct thermodynamic significance. The half-peak potential precedes $E_{1/2}$ by $28.0/n$ mv., or

$$E_{p/2} = E_{1/2} + 1.09(RT/nF) \quad (37)$$

The $E_{1/2}$ value can be estimated from a reversible stationary electrode polarogram from the fact that it occurs at a point 85.17% of the way up the wave.

Calculations based on Equation 33 and also Equation 34 (at least for potentials anodic of $E_{1/2}$) agree exactly with those in Table I, and these data can be used to construct accurate theoretical stationary electrode polarograms.

Cyclic Triangular Wave Method. For the first cycle, the cathodic portion of the polarogram is, of course, the same as described above for the single scan method. However, the height and position of the anodic portion of the polarogram will depend on the switching potential, E_λ, being used.

Polarograms for various values of $(E_\lambda - E_{1/2})n$ were calculated from Equation 31, and, provided that the switching potential is not less than about $35/n$ mv. past the cathodic peak, the curves all have the same relative shape. (For switching potentials close to the peak, the shape of the anodic curve is very dependent on the switching potential, but this is not a usual experimental condition, and will not be considered further.) Typical cyclic polarograms are shown in Figure 2. By using for the base line the cathodic curve which would have been obtained if there had been no change in direction of potential scan, all of the anodic curves are the same, independent of switching potential, and identical in height and shape to the cathodic wave. Thus, when the anodic peak height is measured to the extension of the cathodic curve, the ratio of anodic to cathodic peak currents is unity, independent of the switching potential. This behavior can be used as an important diagnostic criterion to demonstrate the absence (or unimportance) of the various coupled chemical reactions. Of those considered in this paper, only the catalytic case (which can easily be distinguished from the reversible case by other behavior) gives a constant value of unity for the ratio of anodic to cathodic peak height on varying the switching potential. Experimentally, the cathodic base line can be obtained by extending a single scan cathodic sweep beyond the selected switching potential, or if another reaction interferes, by stopping the scan at some convenient potential past the peak, and recording the constant potential current-time curve (using appropriate corrections for charging current). The latter method of obtaining the base line has been proposed for analytical purposes by Reinmuth (*34*).

The position of the anodic wave on the potential axis is a function of the switching potential, especially for small values of $(E_\lambda - E_{1/2})n$. This results from the fact that on the cathodic scan, the surface concentration of substance R does not quite equal Co^* at potentials close to the peak, and if the anodic scan is started under these conditions, $C_R(0, t)$ is slightly less than $Co(0, t)$ was at the corresponding potentials for the cathodic scan. This causes an anodic shift in the wave, which decreases as the switching potential is made more cathodic. The behavior is summarized in Table II.

The transition from the single cycle to the multicycle triangular wave method involves a gradual realignment of concentration gradients at the same relative potentials on successive cycles, which, in turn, causes a gradual change in the shape of both the anodic and cathodic curves. After about 50 cycles (*44*), further changes in shape are very slow, and essentially a steady state cyclic curve is obtained. The relations between the cathodic and anodic peak potentials, peak heights, and switching potentials for the steady state case are given by Matsuda (*22*). Generally, unless a reacting system is being studied, there is little point in investigating the intermediate cyclic scans

beyond the first and before the steady state is reached. Thus, although the individual curves for any number of cycles can be calculated from Equation 31, only the first few have been tabulated for an arbitrarily selected value of E_λ (*27*) and copies of these data are available on request.

II. IRREVERSIBLE CHARGE TRANSFER

Boundary Value Problem. For the case of a totally irreversible reduction taking place at a plane electrode

$$O + ne \xrightarrow{k} R \qquad \text{(II)}$$

the boundary value problem for stationary electrode polarography is similar to the reversible case and Equations 1, 3, 4, and 5a are applicable, except the terms involving substance R are not used. However, Equation 5b is replaced by

$$t > 0, x = 0;\ D_O\left(\frac{\partial C_O}{\partial x}\right) = k\,C_O \qquad (38)$$

Table II. Anodic Peak Potential as a Function of Switching Potential for Reversible Charge Transfer (Case I)

$(E_{1/2} - E_\lambda)n$ mv.	$[E_p(\text{anodic}) - E_{1/2}]n$ mv.
−65	34.4
70	33.7
75	33.3
80	32.9
−100	32.0
150	30.7
200	29.8
300	29.3

where

$$k = k_s \exp[(-\alpha n_a F/RT)(E - E^\circ)] \qquad (39)$$

and the other terms have their usual significance (*5*). In addition, only Equation 6a is required to describe the potential variation, since there is no anodic current on the reverse scan. Thus, the last boundary condition can be written

$$f(t) = D_O\left(\frac{\partial C_O}{\partial x}\right) = C_O k_i e^{bt} \qquad (40)$$

where

$$k_i = k_s \exp[(-\alpha n_a F/RT)(E_i - E^\circ)] \qquad (41)$$

$$b = \alpha n_a F v/RT \qquad (42)$$

Here k_i is the rate constant at the initial potential, and b is analogous to its counterpart a for the reversible case. Using exactly the same methods as above, this boundary value problem can be converted to a single integral equation, first given by Delahay (*4*)

$$1 - \int_0^{bt} \frac{\chi(z)dz}{\sqrt{bt - z}} = (e^{u-bt})\chi(bt) \qquad (43)$$

where

$$e^u = \sqrt{\pi D_O b}/k_i = (\sqrt{\pi D_O b}/k_s) \times \exp[(\alpha n_a F/RT)(E_i - E^\circ)] \qquad (44)$$

For a particular value of u, the solution to Equation 43 provides values of $\chi(bt)$ as a function of bt, which in turn are related to the potential by

$$bt = (\alpha n_a F/RT)(E_i - E) \qquad (45)$$

Provided u is greater than about 7 (which corresponds to selecting an initial potential anodic of the foot of the wave) the values of $\chi(bt)$ are independent of u (*4*). With respect to the initial potential, however, the entire wave shifts along the potential axis as a function of u. Experimentally, the initial potential is a convenient reference point, since E° is seldom known for a totally irreversible system, and data calculated for a particular value of u can be used for any initial potential by arbitrarily shifting the potential axis. For tabulation of data, however, it is more convenient to define a potential axis which will be independent of an arbitrary function such as u, and this can be done by utilizing the relation

$$(E - E^\circ)\alpha n_a + (RT/F)\ln(\sqrt{\pi D_O b}/k_s) = (RT/F)(u - bt) \qquad (46)$$

Thus, values of $\chi(bt)$ can be used to calculate the current

$$i = nFAC_O^* \sqrt{\pi D_O b}\ \chi(bt) \qquad (47)$$

as a function of the potential, which in turn is defined by the left-hand side of Equation 46. Equation 43 is a Volterra integral equation of the second kind, and was evaluated numerically by Delahay (*4*) and also by Matsuda and Ayabe (*23*). The numerical approach described in this paper also is applicable. In addition, a series solution has been reported (*32*)

$$\chi(bt) = \frac{1}{\sqrt{\pi}} \sum_{j=1}^{\infty} (-1)^{j+1} \frac{(\sqrt{\pi})^j}{\sqrt{(j-1)!}} \times \exp\left[\left(-\frac{j\alpha n_a F}{RT}\right)\left(E - E^\circ + \frac{RT}{\alpha n_a F}\ln\frac{\sqrt{\pi D_O b}}{k_s}\right)\right] \qquad (48)$$

The series in Equation 48 is strictly applicable only for values of $bt \geq 4$—i.e., potentials about $100/\alpha n_a$ millivolts cathodic of the initial potential. This is not a serious restriction, and the series is properly convergent over the entire range of interest. Although the series converges very slowly near the peak of the wave, Equation 48 is probably the best way to calculate the current. Since precise values of $\chi(bt)$ have not been published previously, Equation 43 was evaluated using the numerical method, and in addition, values of $\chi(bt)$ were calculated from Equation 48. The results (Table III) were identical and agreed well with the less accurate data previously presented by Delahay (*4*) and Matsuda and Ayabe (*23*). These values of $\chi(bt)$ were calculated using $\delta = 0.01$, with $u = 7.0$, and are accurate to ±0.001.

Table III. Current Functions $\sqrt{\pi}\chi(bt)$ for Irreversible Charge Transfer (Case II)

Potential,[a] mv.	$\sqrt{\pi}\chi(bt)$	$\phi(bt)$	Potential,[a] mv.	$\sqrt{\pi}\chi(bt)$	$\phi(bt)$
160	0.003	0	15	0.437	0.323
140	0.008		10	0.462	0.396
120	0.016		5	0.480	0.482
110	0.024		0	0.492	0.600
100	0.035		− 5	0.496	0.685
90	0.050	0	− 5.34	0.4958	0.694
80	0.073	0.004	10	0.493	0.755
70	0.104	0.010	15	0.485	0.823
60	0.145	0.021	20	0.472	0.895
50	0.199	0.042	25	0.457	0.952
40	0.264	0.083	−30	0.441	0.992
35	0.300	0.115	35	0.423	1.00
30	0.337	0.154	40	0.406	
25	0.372	0.199	50	0.374	
20	0.406	0.253	70	0.323	

[a] The potential scale is $(E - E^\circ)\alpha n_a + (RT/F)\ln\sqrt{\pi D_O b}/k_s$. The initial potential for any value of u can be obtained from $(E - E_i)\alpha n_a = (E - E^\circ)\alpha n_a - (RT/F)(u - \ln\sqrt{\pi D_O b}/k_s)$.

To calculate the current: (1) $i = i(\text{plane}) + i(\text{spherical correction})$
(2) $= nFA\sqrt{bD_O}\,C_O^*\sqrt{\pi}\chi(bt) + nFAD_OC_O^*(1/r_o)\phi(bt)$
(3) $= 602\,n(\alpha n_a)^{1/2}A\sqrt{D_O v}C_O^*[\sqrt{\pi}\chi(bt) + 0.160(\sqrt{D_O}/r_o\sqrt{\alpha n_a v})\phi(bt)]$

Units for (3) are same as Table I.

Table IV. Boundary Value Problems for Stationary Electrode Polarography with Coupled Chemical Reactions

	Reaction	Diffusion Equations	Initial Conditions $t = 0,\ x \geq 0$	Boundary Conditions $t > 0,\ x \to \infty$	Boundary Conditions $t > 0,\ x = 0$
III	$Z \underset{k_b}{\overset{k_f}{\rightleftharpoons}} O$ $O + ne \rightleftharpoons R$	$\frac{\partial C_Z}{\partial t} = D_Z \frac{\partial^2 C_Z}{\partial x^2} - k_f C_Z + k_b C_O$ $\frac{\partial C_O}{\partial t} = D \frac{\partial^2 C_O}{\partial x^2} + k_f C_Z - k_b C_O$ $\frac{\partial C_R}{\partial t} = D_R \frac{\partial^2 C_R}{\partial x^2}$	$C_O/C_Z = K$ $C_O + C_Z = C^*$ $C_R = C_R^*$ $(\approx O)$	$C_O/C_Z \to K$ $C_O + C_Z \to C^*$ $C_R \to O$	$D_Z \frac{\partial C_Z}{\partial x} = O$ $D_O \frac{\partial C_O}{\partial x} = -D_R \frac{\partial C_R}{\partial x}$ $C_O/C_R = \Theta S_\chi(t)$
IV	$Z \underset{k_b}{\overset{k_f}{\rightleftharpoons}} O$ $O + ne \xrightarrow{k} R$	Same as III [a]	Same as III [a]	Same as III [a]	$D_Z \frac{\partial C_Z}{\partial x} = O$ $D_O \frac{\partial C_O}{\partial x} = kC_O = k_i C_O \exp(bt)$
V	$O + ne \rightleftharpoons R$ $R \underset{k_b}{\overset{k_f}{\rightleftharpoons}} Z$	$\frac{\partial C_O}{\partial t} = D_O \frac{\partial^2 C_O}{\partial x^2}$ $\frac{\partial C_R}{\partial t} = D_R \frac{\partial^2 C_R}{\partial x^2} - k_f C_R + k_b C_Z$ $\frac{\partial C_Z}{\partial t} = D_Z \frac{\partial^2 C_Z}{\partial x^2} + k_f C_R - k_b C_Z$	$C_O = C_O^*$ $C_R = C_R^*$ $(\approx O)$ $C_Z = KC_R^*$ $(\approx O)$	$C_O \to C_O^*$ $C_R \to O$ $C_Z \to O$	$D_O \frac{\partial C_O}{\partial x} = -D_R \frac{\partial C_R}{\partial x}$ $D_Z \frac{\partial C_Z}{\partial x} = O$ $C_O/C_R = \Theta S_\chi(t)$
VI	$O + ne \rightleftharpoons R$ $R \xrightarrow{k_f} Z$	$\frac{\partial C_O}{\partial t} = D_O \frac{\partial^2 C_O}{\partial x^2}$ $\frac{\partial C_R}{\partial t} = D_R \frac{\partial^2 C_R}{\partial x^2} - k_f C_R$	Same as V [b]	Same as V [b]	Same as V [b]
VII	$O + ne \rightleftharpoons R$ $R + Z \xrightarrow{k_f'} O$	$\frac{\partial C_O}{\partial t} = D_O \frac{\partial^2 C_O}{\partial x^2} + k_f C_R$ $\frac{\partial C_R}{\partial t} = D_R \frac{\partial^2 C_R}{\partial x^2} - k_f C_R$	Same as Equation 3	Same as Equation 4	Same as Equations 5a and 7
VIII	$O + ne \xrightarrow{k} R$ $R + Z \xrightarrow{k_f'} O$	Same as VII	Same as Equation 3 [a]	Same as Equation 4 [a]	Same as Equation 40

[a] Since the charge transfer is totally irreversible, those equations involving substance R are not used.
[b] Since the chemical reaction is irreversible, the equations involving substance Z are not used.

Experimental Correlations. The relation between the peak potential and the other experimental parameters can be derived from Table III

$$(E_p - E^\circ)\alpha n_a + (RT/F) \ln \sqrt{\pi D_O b}/k_s = -5.34 \text{ mv.} \quad (49)$$

which can be rearranged to obtain

$$E_p = E^\circ - (RT/\alpha n_a F)(0.780 + \ln \sqrt{D_O b} - \ln k_s) \quad (50)$$

This was first derived by Delahay (*4*, *6*) (but note typographical error) and later by Matsuda and Ayabe (*23*). The half-peak potential also can be used as a reference point, and from Table III

$$(E_{p/2} - E^\circ)\alpha n_a + (RT/F) \ln \sqrt{\pi D_O b}/k_s = 42.36 \text{ mv.} \quad (51)$$

Thus,

$$E_p - E_{p/2} = -1.857(RT/\alpha n_a F) \quad (52)$$

From Equations 50 and 52, both the peak potential and the half-peak potential are functions of the rate of potential scan

$$(E_{p/2})_2 - (E_{p/2})_1 = (E_p)_2 - (E_p)_1 = (RT/\alpha n_a F) \ln \sqrt{v_1/v_2} \quad (53)$$

and thus, for a totally irreversible wave, there is a cathodic shift in peak potential or half-peak potential of about $30/\alpha n_a$ millivolts for each ten-fold increase in the rate of potential scan.

An alternate form of Equation 50 also can be derived by combining Equations 40, 44, and 45 with the value of $\chi(bt)$ at the peak, to obtain

$$(C_O)_p/C_O^* = \chi(bt)_p \times \exp\left[(-\alpha n_a F/RT)(E_p - E^\circ + \frac{RT}{\alpha n_a F} \ln \sqrt{\pi D_O b}/k_s)\right] = 0.227 \quad (54)$$

This result does not depend on the other experimental parameters (such as v) and Equation 54 can be solved for the surface concentration of substance O at the peak. This can be substituted into the Eyring equation for a totally irreversible reaction (*5*) to obtain a result first derived by Gokhshtein (*12*) (with a slightly higher constant):

$$i_p = 0.227\, nFAC_O^* k_s \times \exp\left[(-\alpha n_a F/RT)(E_p - E^\circ)\right] \quad (55)$$

Thus, a plot of $\ln(i_p)$ *vs.* $E_p - E^\circ$ (or $E_{p/2} - E^\circ$) for different scan rates would be a straight line with a slope proportional to αn_a, and an intercept proportional to k_s. This appears to be an extremely convenient method of determining the kinetic parameters for this case, although the scan rate would have to be varied over several orders of magnitude.

Still another approach to obtaining kinetic information from stationary electrode polarograms was described by Reinmuth (*30*) who showed that for an irreversible reaction, the current flowing at the foot of the wave is independent of the rate of voltage scan. This same conclusion can be drawn by combining Equations 46 to 48, and considering the first few terms of the series

$$i = nFAC_O^* \sqrt{\pi D_O b}\ [e^{bt-u} - \sqrt{\pi}\, e^{2(bt-u)} + \ldots] \quad (56)$$

The current will be independent of v [note definition of exp (u), Equation 44] when the second term is small compared to the first, or to the 5% error level, when $\sqrt{\pi}$ exp $(bt - u) \leqslant 0.05$. This condition holds for values of $\sqrt{\pi}\chi(bt)$ less than about 0.05, or about 10% of the peak value. Thus, the range of applicability of this useful criterion of irreversibility does not extend as high along the wave as implied by Reinmuth (*30*). For those cases where the second term can be dropped, however, Equation 56 reduces to

$$i = nFAC_O^* k_s \times \exp\ [(-\alpha n_a F/RT)(E - E_i)] \quad (57)$$

and offers a simple way of obtaining kinetic data.

Spherical Electrodes. For an irreversible reaction taking place at a spherical electrode, Reinmuth was able to derive a series solution which is convergent over the entire potential range of interest (*32*). Unfortunately, it is not possible to separate the spherical correction term from the expression for the plane electrode as for the reversible system (Case I). Since the series converges very slowly at potentials near the peak, making the use of a computer almost mandatory, an alternate means of expressing the spherical contribution to the current was sought. A large number of curves were calculated, and the spherical correction—i.e., the difference between the current obtained at spherical and plane electrodes of the same area under identical conditions—was plotted as a function of the dimensionless parameter $\sqrt{D_O}/(r_0\sqrt{b})$ where r_0 is the radius of the electrode. The plot was linear (to better than 1%) for values of $\sqrt{D_O}/(r_0\sqrt{b})$ less than 0.1. Since this includes all values which are of practical use, an irreversible spherical correction term, $\phi(bt)$ was evaluated which can be used just as the analogous term for the reversible case. These values of $\phi(bt)$ are listed in Table III, and values of the current calculated in this way agree well with the considerably less convenient data presented previously (*8*).

COUPLED CHEMICAL REACTIONS

If a homogeneous chemical reaction is coupled to the charge transfer reaction, stationary electrode polarography provides an extremely powerful method of investigating the kinetic parameters. Several of the important kinetic systems are discussed in this work, including those which involve first order (or pseudo first order) preceding, following, or catalytic chemical reactions. Several other cases, including the chemical reaction coupled between two charge transfer reactions, have also been considered, and will be presented elsewhere.

For each of the kinetic cases, the boundary value problem was formulated in a manner similar to Case I or Case II (depending on the nature of the charge transfer reaction) but modified to reflect the kinetic complication. These boundary value problems are presented in Table IV. In each case the rate constant is first order or pseudo first order—e.g., in Cases VII and VIII it was assumed that $C_Z \gg C_O$, and the rate constant which was used in the calculations was $k_f\ (= k_f' C_Z)$. Using the same procedure as outlined in Equations 12 through 22, each of these boundary value problems was converted to a single integral equation. However, in all the kinetic cases except Case VI, at least one of the differential equations involved two concentration variables. Thus, in order to simplify the problem, the usual changes in variable were made (*20*).

The integral equation obtained for each case is presented in Table V. All terms in these equations have been defined previously, except K, which is the equilibrium constant for the chemical reaction, and l which is the sum of the rate constants $(k_f + k_b)$. Each of these integral equations was then solved numerically using the approach described in Equations 26 to 31. Only two different kernels are involved in all the integral equations, and once the procedures were worked out for one case, they could be extended readily to the other cases.

These numerical results (presented in the various tables) provided values of the current functions $\chi(at)$ or $\chi(bt)$ which could be related to potential by Equations 23 and 24 for reversible

Table V. Integral Equations for Stationary Electrode Polarography with Coupled Chemical Reactions

III $$1 - \int_0^{at} \frac{\chi(z)dz}{\sqrt{at - z}} = \frac{1+K}{K} \circledast S_{a\lambda}(at) \int_0^{at} \frac{\chi(z)dz}{\sqrt{at - z}} + \frac{1}{K} \int_0^{at} \frac{e^{-(l/a)(at-z)}\chi(z)dz}{\sqrt{at - z}} \quad (58)$$

IV $$1 - \int_0^{bt} \frac{\chi(z)dz}{\sqrt{bt - z}} = \frac{1+K}{K} e^{u-bt}\chi(bt) + \frac{1}{K} \int_0^{bt} \frac{e^{-(l/b)(bt-z)}\chi(z)dz}{\sqrt{bt - z}} \quad (59)$$

V $$1 - \int_0^{at} \frac{\chi(z)dz}{\sqrt{at - z}} = \frac{1}{1+K} \circledast S_{a\lambda}(at) \int_0^{at} \frac{\chi(z)dz}{\sqrt{at - z}} + \frac{K}{1+K} \circledast S_{a\lambda}(at) \int_0^{at} \frac{e^{-(l/a)(at-z)}\chi(z)dz}{\sqrt{at - z}} \quad (60)$$

VI $$1 - \int_0^{at} \frac{\chi(z)dz}{\sqrt{at - z}} = \gamma \circledast S_{a\lambda}(at) \int_0^{at} \frac{e^{-(k_f/a)(at-z)}\chi(z)dz}{\sqrt{at - z}} \quad (61)$$

VII $$1 - \int_0^{at} \frac{e^{-(k_f/a)(at-z)}\chi(z)dz}{\sqrt{at - z}} = \circledast S_{a\lambda}(at) \int_0^{at} \frac{e^{-(k_f/a)(at-z)}\chi(z)dz}{\sqrt{at - z}} \quad (62)$$

VIII $$1 - \int_0^{bt} \frac{e^{-(k_f/b)(bt-z)}\chi(z)dz}{\sqrt{bt - z}} = e^{u-bt}\chi(bt) \quad (63)$$

charge transfers, and Equations 45 and 46 for irreversible charge transfers.

In each case, the integral equation was made dimensionless by the same substitution (Equation 21), and as a result, the current always can be calculated from the current function $\chi(at)$ or $\chi(bt)$ merely by multiplication by the term $nFAC_0^* \sqrt{\pi D_0 a}$ for reversible charge transfers, or by $nFAC_0^* \sqrt{\pi D_0 b}$ for irreversible charge transfers, as in Equations 25 and 47. [Note that for the preceding chemical reaction (Cases III and IV), the stoichiometric concentration C^* appears in these equations rather than the equilibrium concentration C_0^*.]

For the cases involving an irreversible chemical reaction, no additional restrictions—other than that of selecting an initial potential anodic of the foot of the wave—were introduced in the derivation. For the three cases involving reversible chemical reactions, however, (Cases III, IV, and V) a simplifying assumption was made in order to reduce the number of variables. In these cases, the integrals which arise corresponding to that in Equation 28 are of the form

$$(\sqrt{\delta}/K) \int_0^n \frac{\exp[(\delta\psi)(n-\nu)]\chi(\delta\nu)d\nu}{\sqrt{n-\nu}}$$

for preceding chemical reactions, and

$$K\sqrt{\delta} \int_0^n \frac{\exp[(\delta\psi)(n-\nu)]\chi(\delta\nu)d\nu}{\sqrt{n-\nu}}$$

for succeeding chemical reactions. Here ψ is l/a for reversible charge transfer and l/b for irreversible charge transfer. With these integrals, the integration by parts (used to remove the point of singularity) produces terms of the form

$$(\sqrt{\pi}/K\sqrt{\psi}) \text{ erf } \sqrt{\delta\psi(n-\nu)}$$

for a preceding chemical reaction, and

$$(K\sqrt{\pi}/\sqrt{\psi}) \text{ erf } \sqrt{\delta\psi(n-\nu)}$$

for a succeeding chemical reaction. Although the numerical evaluation could have been carried out retaining all these terms, considerable simplification resulted in assuming that $\delta\psi(n-\nu) \geq 4$. This assumption makes it possible to consider the erf terms as unity, but excludes the cases involving small ψ from the numerical data—i.e., cases where the chemical reaction has no effect on the charge transfer.

These restrictions, once noted, are relatively unimportant and will be discussed in connection with the individual cases. The simplification which results, however, is extremely important. In some previous treatments (*41*) involving reversible chemical reactions, it has been necessary to select a specific value of the equilibrium constant in order to calculate a set of data for a range of rate constants. In this case, for example, a table comparable to Table VII would be required for each value of K likely to be of interest. However, the simplification discussed above makes it possible for the effect of the equilibrium constant on the shape of the polarograms to be separated from its effect on the location of the curve on the potential axis. This can be seen in Equations 58 and 60 where the effect on the potential can be handled by defining a new potential axis in terms of $(E - E_{1/2})n - (RT/F) \ln K/(1+K)$ for Case III and $(E - E_{1/2})n - (RT/F) \ln (1 + K)$ for Case V. For Case IV (Equation 59) the new potential axis is defined in terms of $(E - E^\circ)\ \alpha\ n_a + (RT/F) \ln \sqrt{\pi D_0 b}/k_s - (RT/F) \ln K/(1 + K)$. The effect of K on the shape of the polarograms is included in the numerical data. This approach places no restrictions on the value of the equilibrium constant, and the only exception to the applicability of the numerical data is that stated above: the sum of the rate constants cannot be small compared to a.

The values of $\chi(at)$ and $\chi(bt)$ were calculated using $\delta = 0.02$, and are accurate to $+0.000$, -0.002—i.e., if any error is present, the values tend to be slightly low. The use of a larger value of δ also introduces a small error in the potential, and for each case where the kinetic case reduces to Case I, the waves are shifted cathodic by a few tenths of a millivolt in comparison to Table I.

A series solution also was obtained for each kinetic case (Table VI). As noted previously, only in those cases involving irreversible charge transfer was it possible to obtain series solutions which converged properly over the entire potential range of interest. However, even when unsuitable for calculation of theoretical current voltage curves, the series solutions were extremely useful in correlation of the experimental and kinetic parameters. This was particularly true in those cases in which the series was of the same type as obtained for Cases I or II, since then the form of the solution was known, and correlations

Table VI. Series Solutions for Stationary Electrode Polarography with Coupled Chemical Reactions

III $$\chi(at) = \frac{1}{\sqrt{\pi}} \sum_{j=1}^{\infty} (-1)^{j+1} \left[\sqrt{1} \prod_{i=1}^{j-1} \left(1 + \frac{\sqrt{1}}{K\sqrt{(1/a)+1}}\right)\right] \exp\left[-\frac{jnF}{RT}\left(E - E_{1/2} - \frac{RT}{nF} \ln \frac{K}{1+K}\right)\right] \quad (64)$$

IV $$\chi(bt) = \frac{1}{\sqrt{\pi}} \sum_{j=1}^{\infty} (-1)^{j+1} \left[\frac{(\sqrt{\pi})^j}{\sqrt{(j-1)!}} \prod_{i=1}^{j-1} \left(1 + \frac{\sqrt{1}}{K\sqrt{(1/b)+1}}\right)\right] \exp\left[-\frac{j\alpha n_a F}{RT}\left(E - E^\circ + \frac{RT}{\alpha n_a F} \ln \frac{\sqrt{\pi D b}}{k_s} - \frac{RT}{\alpha n_a F} \ln \frac{K}{1+K}\right)\right] \quad (65)$$

V $$\chi(at) = \frac{1}{\sqrt{\pi}} \sum_{j=1}^{\infty} (-1)^{j+1} \left[\sqrt{1} \Big/ \prod_{i=1}^{j} \left(1 + \frac{K\sqrt{1}}{\sqrt{(1/a)+1}}\right)\right] \exp\left[-\frac{jnF}{RT}\left(E - E_{1/2} - \frac{RT}{nF} \ln(1+K)\right)\right] \quad (66)$$

VI $$\chi(at) = \frac{1}{\sqrt{\pi}} \sum_{j=1}^{\infty} (-1)^{j+1} \left[\frac{1}{\sqrt{(j-1)!}} \prod_{i=1}^{j} \sqrt{(k_f/a)+1}\right] \exp\left[-\frac{jnF}{RT}(E - E_{1/2})\right] \quad (67)$$

VII $$\chi(at) = \frac{1}{\sqrt{\pi}} \sum_{j=1}^{\infty} (-1)^{j+1} \sqrt{(k_f/a)+1}\ \exp\left[-\frac{jnF}{RT}(E - E_{1/2})\right] \quad (68)$$

VIII $$\chi(bt) = \frac{1}{\sqrt{\pi}} \sum_{j=1}^{\infty} (-1)^{j+1} \left[(\sqrt{\pi})^j \Big/ \prod_{i=1}^{j-1} \sqrt{(k_f/b)+1}\right] \exp\left[-\frac{j\alpha n_a F}{RT}\left(E - E^\circ + \frac{RT}{\alpha n_a F} \ln \frac{\sqrt{\pi D b}}{k_s}\right)\right] \quad (69)$$

Table VII. Current Functions $\sqrt{\pi}\chi(at)$ for a Chemical Reaction Preceding a Reversible Charge Transfer (Case III)

Potential[a]	$\sqrt{a}/K\sqrt{l}$ 0.2	0.5	1.0	1.5	3.0	6.0	10.0
120	0.009	0.009	0.009	0.009	0.009	0.009	0.008
100	0.019	0.019	0.019	0.019	0.018	0.017	0.015
80	0.041	0.040	0.039	0.038	0.035	0.031	0.027
60	0.081	0.080	0.075	0.072	0.063	0.051	0.041
50	0.113	0.108	0.100	0.094	0.080	0.062	0.049
45	0.132	0.125	0.116	0.108	0.089	0.068	0.052
40	0.152	0.144	0.131	0.121	0.099	0.074	0.055
35	0.174	0.164	0.149	0.135	0.109	0.079	0.059
30	0.199	0.184	0.164	0.150	0.118	0.084	0.062
25	0.224	0.206	0.183	0.164	0.127	0.089	0.064
20	0.249	0.228	0.199	0.178	0.136	0.093	0.067
15	0.275	0.249	0.216	0.191	0.144	0.098	0.069
10	0.301	0.270	0.232	0.204	0.151	0.101	0.071
5	0.324	0.289	0.246	0.215	0.158	0.104	0.072
0	0.345	0.307	0.259	0.225	0.163	0.107	0.074
−5	0.364	0.321	0.271	0.234	0.168	0.109	0.075
10	0.379	0.334	0.280	0.241	0.173	0.111	0.076
15	0.391	0.344	0.288	0.247	0.176	0.113	0.077
20	0.399	0.351	0.293	0.252	0.179	0.114	0.077
25	0.404	0.355	0.297	0.255	0.181	0.115	0.078
−30	0.406	0.358	0.299	0.257	0.182	0.116	0.078
35	0.405	0.358	0.300	0.258	0.183	0.116	0.079
40	0.402	0.357	0.300	0.258	0.183	0.117	0.079
45	0.397	0.353	0.298	0.258	0.183	0.117	0.079
50	0.390	0.349	0.296	0.256	0.183	0.117	0.079
−60	0.373	0.338	0.289	0.252	0.181	0.116	0.079
80	0.337	0.310	0.272	0.240	0.176	0.115	0.078
100	0.301	0.284	0.253	0.227	0.170	0.113	0.077
120	0.273	0.260	0.236	0.214	0.164	0.110	0.076
140	0.250	0.240	0.222	0.203	0.158	0.108	0.075
$E_{p/2}$, mv.	+29.3	31.3	34.4	37.5	44.2	53.4	62.2

[a] Potential scale is $(E - E_{1/2})n - (RT/F) \ln K/(1 + K)$.

between the potential and kinetic parameters could be obtained from the exponential terms.

III. CHEMICAL REACTION PRECEDING A REVERSIBLE CHARGE TRANSFER

A large group of coupled chemical reactions involves cases in which the electroactive species is produced by a homogeneous first-order chemical reaction preceding a reversible charge transfer

$$Z \underset{k_b}{\overset{k_f}{\rightleftarrows}} O \qquad O + ne \rightleftarrows R \qquad \text{(III)}$$

Only the case in which the chemical reaction is reversible is relevant; however, there are no restrictions on possible values of the equilibrium constant.

This case has been discussed (for the single scan method only) by Saveant and Vianello (*38, 41*), and in addition, a series solution has been presented (*46*).

Qualitatively, the effect of a preceding chemical reaction on the cathodic scan depends on several factors, and three distinct limiting cases can be recognized. First, if l/a is very small, the experiment is over before significant conversion of Z to O can take place. Under such circumstances, the curve obtained is the same shape as Case I, appears at the normal potential for the uncomplicated reduction of O to R, but the magnitude of the current is proportional to the equilibrium concentration of substance O in the bulk of the solution, rather than its stoichiometric concentration C^*. This result can be obtained from Equation 64, which, if l/a is small, reduces to

$$\chi(at) = \frac{1}{\sqrt{\pi}} \sum_{j=1}^{\infty} (-1)^{j+1} \sqrt{j} \left(\frac{K}{1+K}\right) \times \exp[(-jnF/RT)(E - E_{1/2})] \qquad (70)$$

This series is the same as Equation 34 for the reversible case, except for the factor $K/(K + 1)$. If K is large (equilibrium favoring O) a normal stationary electrode polarogram is obtained. On the other hand, if K is small, the current is determined by the equilibrium concentration $C_O^* = [K/(K + 1)]C^*$. This is the one correlation which was not obtained from the numerical solution, because of the simplifying assumption (that l/a is not very small) which was made in the derivation. This restriction is not particularly serious, however, because the option of varying the rate of potential scan lends great versatility to the method. For example, if low values of l/a are encountered experimentally, and reasonable values of l are involved, one could merely reduce the rate of voltage scan to a region where the numerical data are applicable. On the other hand, if l is low and a has already been reduced to the lower practical limit, Equation 70 could be used directly to calculate the theoretical current potential curve. The converse approach, of using large enough rates of voltage scan to ensure that this condition holds, has been used by Papoff to determine equilibrium constants (*28*).

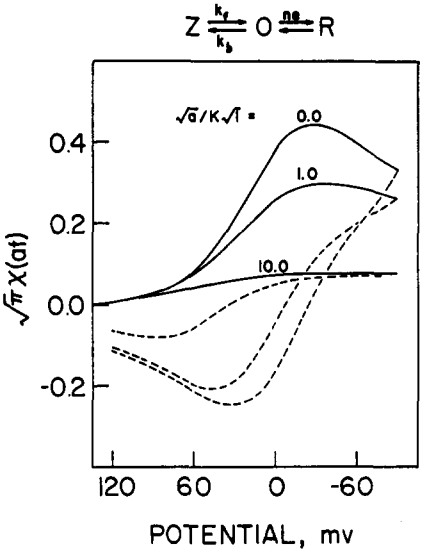

Figure 3. Cyclic stationary electrode polarograms (Case III)

Potential scale is $(E - E_{1/2})n - (RT/F)\ln K/(1 + K)$

The two other limiting cases can be obtained from Equation 64 by assuming first that l/a is large, so that $l/a + i \approx l/a$, and then considering either large or small values of $\sqrt{a}/K\sqrt{l}$. If $\sqrt{a}/K\sqrt{l}$ is small, Equation 64 reduces to

$$\chi(at) = \frac{1}{\sqrt{\pi}} \sum_{j=1}^{\infty} (-1)^{j+1} \times \sqrt{j} \exp\left[(-jnF/RT)\left(E - E_{1/2} - \frac{RT}{nF} \ln \frac{K}{1+K}\right)\right] \qquad (71)$$

which is the same as Equation 34 for the reversible case, except that the wave appears at a potential determined by the equilibrium constant. At the other limit, for large values of $\sqrt{a}/K\sqrt{l}$, Equation 64 reduces to

$$\chi(at) = \frac{1}{\sqrt{\pi}} \sum_{j=1}^{\infty} (-1)^{j+1} \sqrt{j!}\, K \sqrt{l/a} \times \exp\left[-\frac{jnF}{RT}\left(E - E_{1/2} - \frac{RT}{nF} \ln \frac{K}{1+K} - \frac{RT}{nF} \ln \frac{\sqrt{a}}{K\sqrt{l}}\right)\right] \qquad (72)$$

This series does not correspond to one of the previously encountered cases, and it cannot be characterized merely by inspection. Nevertheless the appearance of the term $1/\sqrt{a}$ in each

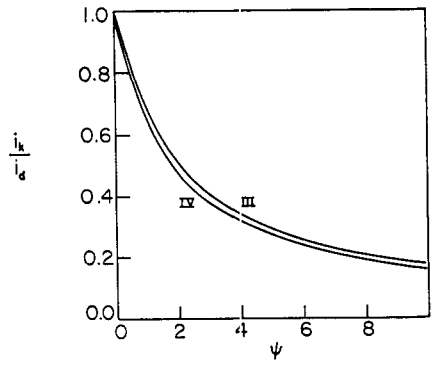

Figure 4. Working curve, ratio of kinetic peak current to diffusion controlled peak current

Case III: $\psi = \sqrt{a}/K\sqrt{l}$
Case IV: $\psi = \sqrt{b}/K\sqrt{l}$

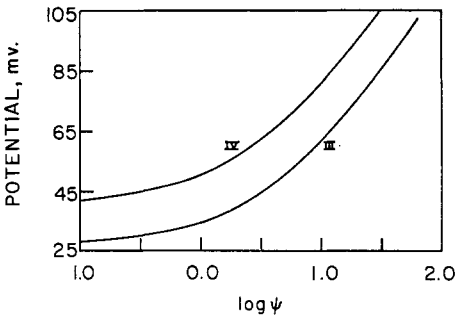

Figure 5. Variation of half-peak potential as a function of the kinetic parameters

Case III: $\psi = \sqrt{a}/K\sqrt{l}$; potential scale is $(E_{p/2} - E_{1/2})n - (RT/F)\ln K/(1 + K)$. Case IV: $\psi = \sqrt{b}/K\sqrt{l}$; potential scale is $(E_{p/2} - E^\circ)\alpha n_a - (RT/F)\ln K/(1 + K) + (RT/F)\ln\sqrt{\pi Db/k_s}$

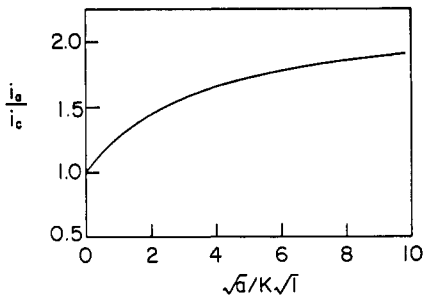

Figure 6. Ratio of anodic to cathodic peak current as a function of kinetic parameters, Case III

term of the sum indicates that the magnitude of the current will be independent of the rate of potential scan.

Single Scan Method. The characteristics of the stationary electrode polarogram between these two limiting cases were obtained from the numerical calculations. Typical cyclic polarograms calculated for several values of $\sqrt{a}/K\sqrt{l}$ are shown in Figure 3. The curve for $\sqrt{a}/K\sqrt{l}$ equal to zero corresponds to the reversible case, and as the chemical step becomes more important, the curves become more drawn out. It should be noted that in Figure 3 the ordinate is $\chi(at)$, and not the current. Thus, for the situation where an increase in $\sqrt{a}/K\sqrt{l}$ corresponds to an increase in a, the current function $\chi(at)$ decreases, but the actual current increases, since the factor $\sqrt{a}$ appears in Equation 25 for the current. In the limit for large values of a, the decrease in $\chi(at)$ exactly balances this factor $\sqrt{a}$ in Equation 25, so that the current becomes independent of a, as indicated in Equation 72.

Values of the rate constants can be obtained from the cathodic stationary electrode polarograms (provided the equilibrium constant is known) by comparing the experimental curves with theoretical plots such as in Figure 3. Data for construction of accurate theoretical polarograms are presented in Table VII.

Since this is a rather cumbersome way of handling the data, an alternate approach may be more convenient. A large number of theoretical curves were calculated for various values of $\sqrt{a}/K\sqrt{l}$, in addition to those listed in Table VII. From these data, a working curve was constructed for the ratio i_k/i_d of the peak current obtained in a kinetic case to that expected for an uncomplicated diffusion controlled case. This procedure makes it unnecessary to have the value of several of the experimental parameters such as the diffusion coefficient, electrode area, etc. The working curve for this case (Figure 4) fits the empirical equation

$$i_k/i_d = \frac{1}{1.02 + 0.471\sqrt{a}/K\sqrt{l}} \quad (73)$$

to about 1% (except for very low values of $\sqrt{a}/K\sqrt{l}$, where the error does not exceed 1.5%). More precise values of the ratio i_k/i_d as a function of $\sqrt{a}/K\sqrt{l}$ have been tabulated (*27*), and if required for construction of a more exact working curve, are available on request.

As indicated from the series solutions, the potential at which the wave appears is independent of $\sqrt{a}/K\sqrt{l}$ for small values (Equation 71) while the wave shifts anodic by about $60/n$ mv. for each ten-fold increase in $\sqrt{a}/K\sqrt{l}$ for large values (Equation 72). For intermediate values, the shift in potential can be obtained from the numerical data. Since the wave is drawn out for large values of $\sqrt{a}/K\sqrt{l}$ in this case, it is more convenient to consider shifts in half peak potential rather than peak potential, and this behavior (Figure 5) can be used to obtain kinetic data.

Cyclic Triangular Wave Method. As shown in Figure 3, the anodic portion of a cyclic stationary electrode polarogram is not affected quite as much by the preceding chemical reaction as is the cathodic portion. For example, for $\sqrt{a}/K\sqrt{l}$ equal to 3.0, the cathodic curve is quite flat, but since the anodic portion involves a chemical reaction after charge transfer, it has many of the characteristics of Case V, and is still markedly peak shaped. For these curves, a switching potential $(E_\lambda - E_{1/2})n - (RT/F)\ln(K/(1 + K))$ of -90 mv. was selected. The shape of the anodic curves is a function of the switching potential, and thus, it is not practical to compile a table of the anodic current function, although such data are available on request (*27*). In general, the height of the anodic peak (as measured to the extension of the cathodic curve) increases as the switching potential is made more cathodic.

The anodic current is fairly insensitive to changes in $\sqrt{a}/K\sqrt{l}$ for values larger than about 5, and thus the range of applicability of this correlation is about the same as for the cathodic current (Figures 3 and 4). However, for those cases where a value of i_d cannot be obtained for use with the working curve of Figure 4, the kinetic parameters can be determined by relating $\sqrt{a}/K\sqrt{l}$ to the ratio of the anodic to cathodic peak currents. A working curve for this correlation is shown in Figure 6. Data for construction of a more accurate working curve are available on request (*27*).

IV. CHEMICAL REACTION PRECEDING AN IRREVERSIBLE CHARGE TRANSFER

The case in which a first order chemical reaction precedes an irreversible charge transfer

$$Z \underset{k_b}{\overset{k_f}{\rightleftharpoons}} O$$
$$O + ne \xrightarrow{k} R \quad \text{(IV)}$$

has not been discussed previously. The stationary electrode polarograms are qualitatively similar to Case III, except, of course, no anodic current is observed in the cyclic triangular wave experiment, and further, the curves are even more drawn out because of the effect of the electron transfer coefficient, α. Thus, although the main effect of the preceding chemical reaction is the same as Case III—i.e., to decrease the current (compared to the irreversible charge transfer without chemical complication)—the detailed characteristics of the two cases are markedly different, and effects of the rate controlled charge transfer can be separated from the rate controlled chemical reaction by quantitative evaluation of the stationary electrode polarograms.

As in Case III, three distinct limiting cases can be considered depending on the kinetic parameter $\sqrt{b}/K\sqrt{l}$.

First, if l/b is small, the curve is the same shape as Case II, its potential is unaffected by the kinetic complication, and the magnitude of the current is a function of the equilibrium concentration of substance O. Thus, for small values of l/b, Equation 65 reduces to

$$\chi(bt) = \frac{1}{\sqrt{\pi}} \sum_{j=1}^{\infty} (-1)^{j+1} \frac{(\sqrt{\pi})^j}{\sqrt{(j-1)!}} \times \left(\frac{K}{1+K}\right) \exp\left[-\frac{j\alpha n_a F}{RT}\left(E - E^\circ + \frac{RT}{\alpha n_a F} \ln \sqrt{\pi Db}/k_s\right)\right] \quad (74)$$

which is the same as Equation 48 for the uncomplicated irreversible case except for the factor $K/(1 + K)$. As in Case III, this is the correlation which is not included in the numerical data because of the simplifying assumptions made.

The two other limiting cases are obtained by assuming first that l/b is large, and then considering the series for both small and large values of $\sqrt{b}/K\sqrt{l}$. If $\sqrt{b}/K\ \sqrt{l}$ is small, Equation 65 reduces to

$$\chi(bt) = \frac{1}{\sqrt{\pi}} \sum_{j=1}^{\infty} (-1)^{j+1} \frac{(\sqrt{\pi})^j}{\sqrt{(j-1)!}} \times \exp\left[-\frac{j\alpha n_a F}{RT}\left(E - E^\circ + \frac{RT}{\alpha n_a F} \ln \frac{\sqrt{\pi Db}}{k_s} - \frac{RT}{\alpha n_a F} \ln \frac{K}{1+K}\right)\right] \quad (75)$$

which is the same as Equation 48 for the irreversible case, except that the potential at which the wave appears has been shifted by the equilibrium constant.

At the other limit, for large values of $\sqrt{b}/K\sqrt{l}$, Equation 65 reduces to

$$\chi(bt) = \frac{1}{\sqrt{\pi}} \sum_{j=1}^{\infty} (-1)^{j+1} (\sqrt{\pi})^j K\sqrt{l/b} \times \exp\left[-\frac{j\alpha n_a F}{RT}\left(E - E^\circ + \frac{RT}{\alpha n_a F} \ln \frac{\sqrt{\pi Db}}{k_s} - \frac{RT}{\alpha n_a F} \ln \frac{K}{1+K} + \frac{RT}{\alpha n_a F} \ln \frac{K\sqrt{\pi b}}{\sqrt{l}}\right)\right] \quad (76)$$

At this limit, a peak is no longer observed, and both the potential of the wave and magnitude of the current are independent of b. In addition, Equation 76 can be written in a closed form valid for large values of $\sqrt{b}/K\ \sqrt{l}$

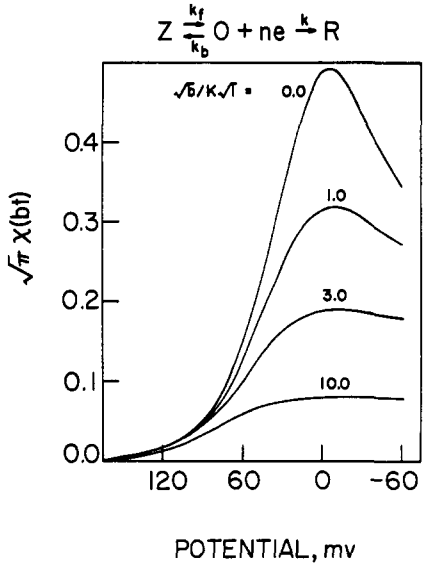

Figure 7. Stationary electrode polarograms, Case IV

Potential scale is $(E - E^\circ)\alpha n_a + (RT/F) \ln \sqrt{\pi Db}/k_s - (RT/F) \ln K/(1 + K)$

$$i = (nFAC^* \sqrt{D}\, K\sqrt{l})/1 + \exp\left[\frac{\alpha n_a F}{RT}\left(E - E^\circ + \frac{RT}{\alpha n_a F} \ln \frac{\sqrt{\pi Db}}{k_s} - \frac{RT}{\alpha n_a F} \ln \frac{K}{1+K} + \frac{RT}{\alpha n_a F} \ln \frac{K\sqrt{\pi b}}{\sqrt{l}}\right)\right] \quad (77)$$

This is the equation for an S-shaped current-voltage curve, and at cathodic potentials the current is directly proportional to the term $K(k_f + k_b)^{1/2}$.

Between these last two limiting cases, the characteristics of the stationary electrode polarogram can be obtained from the numerical solution to Equation 59. Alternatively, theoretical current-potential curves could be calculated from the series solution, Equation 65, which converges properly over the entire potential range. Typical polarograms are given in Figure 7, and data for construction of accurate curves are listed in Table VIII.

As in Case III, the kinetic parameters can be obtained from a direct comparison of experimental and theoretical polarograms, or from working curves of the ratio i_k/i_d of the kinetic peak current to the diffusion controlled peak current for an irreversible charge transfer (Figure 4). The working curve for this case was found to fit the empirical equation

$$i_k/i_d = \frac{1}{1.02 + 0.531\ \sqrt{b}/K\sqrt{l}} \quad (78)$$

The applicability of Equation 78 is about the same as Equation 73.

Table VIII. Current Functions $\sqrt{\pi}\chi(bt)$ for a Chemical Reaction Preceding an Irreversible Charge Transfer (Case IV)

Potential[a]	$\sqrt{b}/K\sqrt{l}$ 0.2	0.5	1.0	1.5	3.0	6.0	10.0
160	0.003	0.003	0.003	0.003	0.003	0.003	0.003
140	0.007	0.007	0.007	0.007	0.007	0.007	0.007
120	0.016	0.016	0.016	0.016	0.015	0.015	0.014
110	0.024	0.024	0.023	0.023	0.022	0.021	0.019
100	0.035	0.034	0.034	0.033	0.031	0.029	0.026
90	0.050	0.049	0.048	0.047	0.044	0.039	0.033
80	0.070	0.070	0.067	0.065	0.059	0.050	0.042
70	0.102	0.099	0.094	0.090	0.079	0.063	0.050
60	0.140	0.134	0.126	0.117	0.100	0.076	0.058
50	0.190	0.179	0.164	0.151	0.122	0.088	0.065
40	0.248	0.230	0.205	0.185	0.143	0.099	0.070
35	0.280	0.257	0.226	0.201	0.152	0.103	0.072
30	0.312	0.282	0.244	0.216	0.161	0.107	0.074
25	0.343	0.307	0.263	0.230	0.168	0.110	0.076
20	0.370	0.330	0.279	0.241	0.174	0.112	0.077
15	0.395	0.349	0.292	0.251	0.179	0.115	0.078
10	0.414	0.364	0.302	0.260	0.183	0.116	0.079
5	0.430	0.375	0.310	0.265	0.186	0.117	0.079
0	0.440	0.382	0.315	0.269	0.188	0.118	0.080
−5	0.444	0.385	0.318	0.271	0.189	0.119	0.080
−10	0.443	0.386	0.318	0.272	0.189	0.119	0.080
15	0.438	0.383	0.317	0.271	0.189	0.119	0.080
20	0.430	0.378	0.314	0.269	0.189	0.119	0.080
25	0.419	0.371	0.310	0.267	0.188	0.119	0.080
30	0.407	0.362	0.306	0.263	0.187	0.118	0.080
−35	0.394	0.354	0.301	0.260	0.186	0.118	0.080
40	0.381	0.345	0.295	0.257	0.184	0.117	0.079
50	0.355	0.327	0.283	0.248	0.180	0.116	0.079
60	0.333	0.309	0.272	0.240	0.177	0.115	0.078
70	0.313	0.294	0.261	0.233	0.174	0.114	0.078
$E_{p/2}$, mv.	+44.2	47.3	51.4	54.5	62.2	71.9	82.2

[a] Potential scale is $(E - E^\circ)\alpha n_a - (RT/F) \ln K/(1 + K) + (RT/F) \ln \sqrt{\pi Db}/k_s$

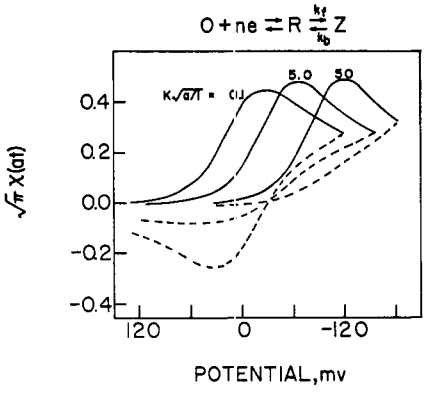

Figure 8. Stationary electrode polarograms, Case V

Potential scale is $(E - E_{1/2})n - (RT/F) \ln (1 + K)$

As indicated from the series solutions, the potential at which the peak appears differs from Case III. The potential does not depend on $\sqrt{b}/K\sqrt{l}$ for small values of the kinetic parameter (Equation 75), while the potential shifts anodic by about $60/\alpha n_a$ mv. for each ten-fold increase for large values of $\sqrt{b}/K\sqrt{l}$ (Equations 76 and 77). This behavior, which also can be used to obtain kinetic data, is contrasted with Case III in Figure 5.

V. CHARGE TRANSFER FOLLOWED BY A REVERSIBLE CHEMICAL REACTION

The case in which a reversible chemical reaction follows a reversible charge transfer

$$O + ne \rightleftharpoons R \qquad R \underset{k_b}{\overset{k_f}{\rightleftarrows}} Z \qquad \text{(V)}$$

includes a fairly large group of organic electrode reactions. Such reactions have been studied by numerous workers using a variety of electrochemical techniques. However, the theory for stationary electrode polarography has not previously been presented.

If the charge transfer is irreversible, a succeeding chemical reaction will have no effect on the stationary electrode polarogram. The chemical reaction can still be studied if either substance R or Z is electroactive at some other potential but such cases will not be considered here, and are probably more easily handled by other techniques such as step functional controlled potential electrolysis (*43*).

Depending on the magnitude of the kinetic parameters, three limiting cases can be distinguished. First, if the rate of the chemical reaction is very fast, the system will be in equilibrium at all times, and the only effect will be an anodic displacement of the wave along the potential axis. This result can be obtained from Equation 66, which for large values of l/a reduces to

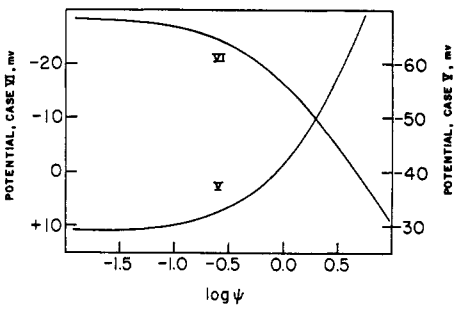

Figure 9. Variation of peak potential as a function of kinetic parameters

Case V: $\psi = K\sqrt{a/l}$; the potential scale is $(E_p - E_{1/2})n - (RT/F) \ln (1 + K)$
Case VI: $\psi = k_f/a$; the potential scale is $(E_p - E_{1/2})n$

$$\chi(at) = \frac{1}{\sqrt{\pi}} \sum_{j=1}^{\infty} (-1)^{j+1} \sqrt{j} \times \exp\left[-\frac{jnF}{RT} \left(E - E_{1/2} - \frac{RT}{nF} \ln (1 + K) \right) \right] \qquad (79)$$

This series is the same as Equation 34 for the reversible case, except for the term $(RT/nF) \ln(1 + K)$ in the exponential, which reflects the anodic displacement of the wave.

The second limiting case to be considered is that in which the chemical reaction is very slow, so that essentially no chemical reaction takes place during the experiment. Under such conditions the curve should again be the normal reversible shape, but should appear at its normal potential. Thus, if l/a is small, Equation 66 reduces exactly to Equation 34. This is the limiting case which is not included in the numerical solution because of the simplifying assumption. Unfortunately this case is important experimentally, particularly when the equilibrium constant is large. Under these circumstances, however, the chemical reaction can be considered irreversible ($k_f \gg k_b$), and an alternate approach to the theory is available. This will be treated as Case VI, below.

The third limiting case occurs when l/a is large, and the kinetic parameter $K\sqrt{a/l}$ also is large. Under these conditions Equation 66 reduces to

$$\chi(at) = \frac{1}{\sqrt{\pi}} \sum_{j=1}^{\infty} (-1)^{j+1} \frac{(\sqrt{\pi})^j}{\sqrt{(j-1)!}} \times \exp\left[-\frac{jnF}{RT} \left(E - E_{1/2} - \frac{RT}{nF} \ln (1 + K) + \frac{RT}{nF} \ln K\sqrt{\pi a/l} \right) \right] \qquad (80)$$

which is the same form as the irreversible series, Equation 48. Thus, a stationary electrode polarogram is obtained which is the same shape as an irreversible curve, $\chi(at)$ at the peak will equal 0.496 (the value of $\chi(bt)$ in Case II), and

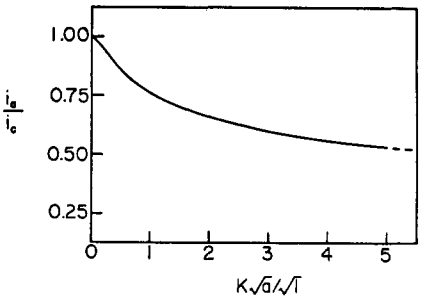

Figure 10. Ratio of anodic to cathodic peak current as a function of the kinetic parameters, Case V

using an approach similar to Equations 49 and 50, it can be shown that

$$E_p = E_{1/2} - (RT/nF)[0.780 + \ln K\sqrt{a/l} - \ln (1 + K)] \qquad (81)$$

In these limiting cases, the peak potential will shift cathodic by about $60/n$ mv. for a ten-fold increase in $K\sqrt{a/l}$.

Single Scan Method. Typical stationary electrode polarograms calculated from Equation 60 are shown in Figure 8 and the data are listed in Table IX. However, the cathodic current function $\chi(at)$ varies only from 0.446 to 0.496 with a variation of three orders of magnitude in $K\sqrt{a/l}$, and thus is not particularly useful for kinetic measurements.

The variation of peak potential with $K\sqrt{a/l}$ is probably more useful for characterizing the kinetic parameters from the cathodic scan. For small values of $K\sqrt{a/l}$, the curves approach reversible behavior (Equation 79) and the potential is independent of $K\sqrt{a/l}$. At the other limit (Equations 80 and 81) the peak potential shifts cathodically by about $60/n$ mv. for a ten-fold increase in $K\sqrt{a/l}$. For intermediate values of $K\sqrt{a/l}$, the variation in peak potential can be obtained from Table IX, and a working curve can be constructed as in Figure 9. Extrapolation of the straight line segments of the data indicate that Equation 79 will hold whenever $K\sqrt{a/l}$ is less than about 0.05, and that Equation 80 (or 81) will hold when $K\sqrt{a/l}$ is larger than about 5.0.

Cyclic Triangular Wave Method. As expected from the mechanism, the anodic portion of the cyclic stationary electrode polarogram is very sensitive to the kinetic parameters (Figure 8). Unfortunately, the peak height also is a function of the switching potential, and thus it is not convenient to compile tables of $\chi(at)$ for the anodic portion of the scan, although such data are available on request (*27*). In order to use the anodic current for kinetic measurements, therefore, it was necessary to select arbitrary switching potentials, and prepare working curves

Table IX. Current Functions $\sqrt{\pi}\chi(at)$ for Charge Transfer Followed by a Reversible Chemical Reaction (Case V)

Potential[a]	$K\sqrt{a/l}$ 0.1	0.25	0.55	1.0	2.0	3.25	5.0	10.0
120	0.008	0.007	0.006	0.005	0.003	0.002	0.002	0.001
100	0.018	0.016	0.013	0.010	0.007	0.005	0.003	0.002
80	0.037	0.034	0.028	0.021	0.015	0.010	0.007	0.004
60	0.079	0.070	0.057	0.046	0.031	0.022	0.016	0.009
50	0.108	0.097	0.082	0.066	0.045	0.032	0.023	0.013
45	0.128	0.115	0.097	0.079	0.054	0.039	0.028	0.016
40	0.149	0.135	0.114	0.093	0.065	0.047	0.034	0.019
35	0.173	0.157	0.134	0.110	0.077	0.056	0.041	0.022
30	0.200	0.182	0.158	0.129	0.092	0.068	0.049	0.028
25	0.227	0.210	0.183	0.152	0.110	0.081	0.059	0.033
20	0.256	0.239	0.210	0.177	0.129	0.096	0.070	0.040
15	0.286	0.269	0.240	0.205	0.151	0.114	0.084	0.048
10	0.316	0.301	0.272	0.235	0.177	0.135	0.099	0.058
5	0.342	0.330	0.303	0.265	0.205	0.159	0.118	0.069
0	0.372	0.359	0.334	0.300	0.236	0.184	0.141	0.083
−5	0.395	0.386	0.364	0.332	0.268	0.213	0.166	0.100
10	0.414	0.408	0.390	0.363	0.302	0.245	0.192	0.118
15	0.430	0.426	0.414	0.391	0.336	0.278	0.222	0.138
20	0.440	0.439	0.433	0.416	0.368	0.313	0.254	0.163
25	0.447	0.448	0.446	0.436	0.398	0.347	0.288	0.189
−30	0.449	0.452	0.455	0.452	0.424	0.380	0.322	0.220
35	0.447	0.452	0.459	0.461	0.446	0.410	0.357	0.252
40	0.443	0.449	0.458	0.465	0.461	0.436	0.392	0.287
45	0.435	0.442	0.453	0.464	0.470	0.455	0.420	0.323
50	0.426	0.433	0.446	0.459	0.474	0.469	0.445	0.358
−55	0.416	0.423	0.436	0.451	0.472	0.478	0.464	0.391
60	0.405	0.412	0.425	0.441	0.446	0.479	0.476	0.422
65	0.393	0.400	0.412	0.429	0.456	0.476	0.483	0.447
70	0.381	0.387	0.400	0.416	0.444	0.467	0.483	0.468
75	0.369	0.376	0.387	0.403	0.431	0.456	0.477	0.480
−80	0.357	0.364	0.375	0.389	0.417	0.443	0.468	0.487
85	0.346	0.352	0.362	0.376	0.402	0.429	0.455	0.487
90	0.336	0.341	0.351	0.363	0.389	0.414	0.440	0.482
95	0.326	0.330	0.339	0.351	0.375	0.399	0.425	0.471
100	0.316	0.320	0.328	0.340	0.362	0.383	0.409	0.458
−110			0.309	0.319	0.337	0.356	0.378	0.427
120					0.316	0.333	0.352	0.395
130						0.312	0.329	0.366
140							0.308	0.340
E_p, mv.	−30.3	−32.4	−36.5	−41.6	−50.9	−59.1	−67.3	−82.7

[a] Potential scale is $(E - E_{1/2})n - (RT/F)\ln(1 + K)$.

of the ratio i_p (anodic) $/i_p$(cathodic) as a function of $K\sqrt{a/l}$. The curve for a switching potential of $(E_\lambda - E_{1/2})n - (RT/F)\ln(1 + K)$ equal to −90 mv. is shown in Figure 10.

VI. CHARGE TRANSFER FOLLOWED BY AN IRREVERSIBLE CHEMICAL REACTION

As indicated above, an alternate approach to the theory of stationary electrode polarography for succeeding chemical reactions—which permits correlations for small values of l/a—involves considering the chemical reaction to be irreversible

$$O + ne \rightleftharpoons R \qquad R \xrightarrow{k_f} Z \qquad \text{(VI)}$$

Except for a brief presentation of a series solution (*32*) the theory of stationary electrode polarography for this case has not been presented previously.

Qualitatively, the behavior is very similar to Case V, except that neither the equilibrium constant nor k_b is included in the kinetic parameter. Thus, for small values of k_f/a, the chemical reaction has little effect, and a reversible stationary electrode polarogram is observed at its normal potential. This result can be obtained from the series solution, since when k_f/a is small Equation 67 reduces to Equation 34. This limiting case is precisely the one not included in the numerical calculations of Case V, but is included here.

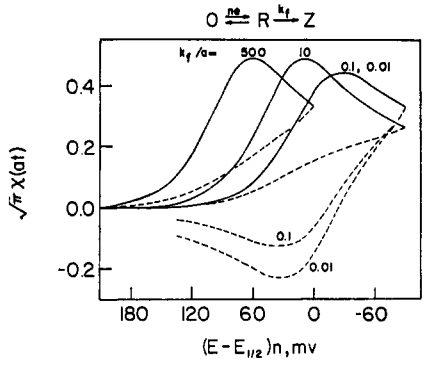

Figure 11. Stationary electrode polarograms, Case VI

At the other limit, as k_f/a becomes large, Equation 67 reduces to

$$\chi(at) = \frac{1}{\sqrt{\pi}} \sum_{j=1}^{\infty} (-1)^{j+1} \frac{(\sqrt{\pi})^j}{\sqrt{(j-1)!}} \times \exp\left[-\frac{jnF}{RT}\left(E - E_{1/2} - \frac{RT}{nF}\ln\sqrt{k_f/a\pi}\right)\right] \qquad (82)$$

which is the same form as the series for the irreversible case (Equation 48). In this case it can be shown that

$$E_p = E_{1/2} - (RT/nF) \times (0.780 - \ln\sqrt{k_f/a}) \qquad (83)$$

Thus, it can be seen that this limiting case is the same one as the third listed under Case V, except that it is approached from the opposite direction. For Equation 83 an increase in the kinetic parameter k_f/a causes an anodic shift in the wave, while for Equation 81, an increase in the kinetic parameter $K\sqrt{a/l}$ causes a cathodic shift in the wave. This is because the term $\ln(1 + K)$ in Equation 81 has already shifted the wave anodic by an amount corresponding to the maximum possible for complete equilibrium.

Single Scan Method. Stationary electrode polarograms calculated from Equation 61 are shown in Figure 11, and the data are presented in Table X. As in Case V, the cathodic cur-

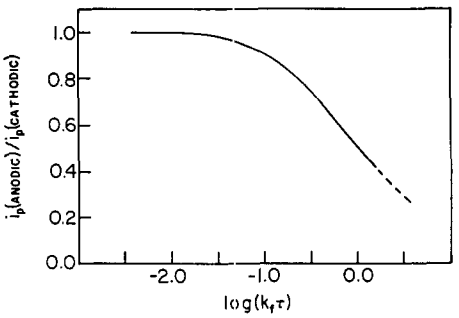

Figure 12. Ratio of anodic to cathodic peak current as a function of $k_f\tau$, Case VI

rents vary by only about 10% for a variation in k_f/a of about three orders of magnitude, and thus are not useful for kinetic measurements. Again, the variation in peak potential is probably more useful. For small values of k_f/a, the peak potential is independent of k_f/a, while for large values, an anodic shift of about $30/n$ mv. for a ten-fold increase in k_f/a is observed. This behavior, and also the behavior for intermediate values of k_f/a are included in Figure 9, and the limits of applicability of Equations 34 and 82 (or 36 and 83) can be estimated as before.

Cyclic Triangular Wave Method. As in Case V, measurements on the anodic portion of the cyclic triangular wave are most suitable for kinetic measurements (Figure 11), but as before the anodic current function depends on the switching potential. In this case, however, an extremely simple way of handling the data was found. A large number of single cycle theoretical curves were calculated varying both k_f/a and the switching potential, and for a constant value of the parameter $k_f\tau$ (where τ is the time in seconds from $E_{1/2}$ to E_λ), the ratio of anodic to cathodic peak currents was found to be constant. (As before, the anodic peak current is measured to the extension of the cathodic curve.) Thus a working curve could be constructed for the ratio of peak currents i_a/i_c as a function of $k_f\tau$ (Figure 12), and if

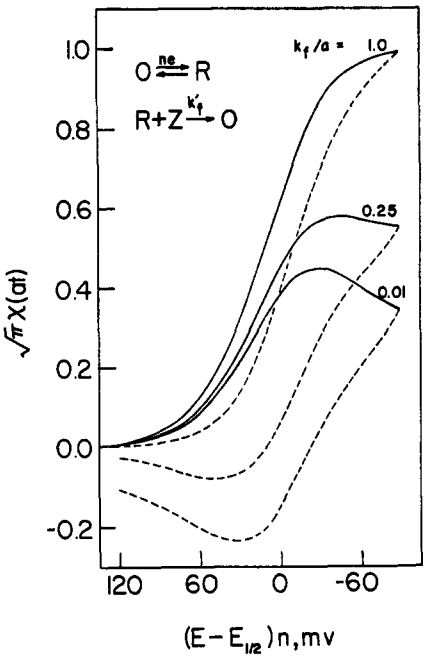

Figure 13. Stationary electrode polarograms, Case VII

$E_{1/2}$ is known, a rate constant can be calculated from a single cyclic curve.

By using faster scan rates (small k_f/a), $E_{1/2}$ also can be obtained experimentally. For accurate work, a large scale plot of Figure 12 would be required, and the data are presented in Table XI.

Qualitatively, from Figure 12, it is very difficult to measure the anodic scan for values of $k_f\tau$ much greater than 1.6. Conversely, a value of $k_f\tau$ much less than 0.02 cannot be distinguished from the reversible case. The method is very convenient, since the ratio of peak heights is independent of such experimental parameters as the electrode area and diffusion coefficient.

VII. CATALYTIC REACTION WITH REVERSIBLE CHARGE TRANSFER

For an irreversible catalytic reaction following a reversible charge transfer,

$$O + ne \rightleftharpoons R \qquad R + Z \xrightarrow{k'_f} O \qquad \text{(VII)}$$

Table X. Current Functions $\sqrt{\pi}\chi(at)$ for Charge Transfer Followed by an Irreversible Chemical Reaction (Case VI)

	k_f/a						
Potential[a]	0.05	0.2	0.5	1.0	1.6	4.0	10.0
160	0.003	0.003	0.003	0.003	0.003	0.004	0.006
150	0.003	0.003	0.004	0.004	0.005	0.006	0.009
140	0.004	0.005	0.005	0.006	0.007	0.009	0.014
130	0.006	0.007	0.008	0.009	0.010	0.014	0.020
120	0.009	0.010	0.011	0.013	0.015	0.020	0.030
110	0.014	0.015	0.016	0.019	0.022	0.030	0.044
100	0.020	0.021	0.024	0.027	0.032	0.043	0.062
90	0.029	0.031	0.035	0.040	0.046	0.062	0.090
80	0.042	0.045	0.050	0.057	0.065	0.089	0.126
70	0.061	0.065	0.072	0.083	0.093	0.124	0.175
65	0.073	0.077	0.085	0.098	0.110	0.147	0.203
60	0.086	0.092	0.101	0.116	0.130	0.173	0.234
55	0.102	0.108	0.120	0.136	0.153	0.200	0.268
50	0.120	0.128	0.141	0.160	0.177	0.230	0.303
45	0.140	0.148	0.163	0.185	0.206	0.263	0.338
40	0.163	0.172	0.189	0.213	0.236	0.297	0.373
35	0.188	0.199	0.218	0.244	0.269	0.332	0.406
30	0.216	0.227	0.248	0.276	0.302	0.367	0.435
25	0.244	0.256	0.278	0.308	0.335	0.398	0.459
20	0.273	0.288	0.310	0.340	0.367	0.427	0.477
15	0.303	0.317	0.341	0.371	0.396	0.451	0.488
10	0.333	0.347	0.371	0.400	0.423	0.469	0.491
5	0.359	0.374	0.396	0.424	0.445	0.480	0.489
0	0.384	0.398	0.419	0.443	0.461	0.486	0.481
−5	0.405	0.418	0.437	0.458	0.472	0.485	0.469
−10	0.423	0.434	0.451	0.467	0.476	0.480	0.455
15	0.435	0.445	0.459	0.471	0.476	0.469	0.439
20	0.444	0.452	0.462	0.470	0.471	0.456	0.422
25	0.448	0.454	0.461	0.464	0.461	0.440	0.405
30	0.448	0.452	0.457	0.456	0.450	0.424	0.389
−35	0.445	0.448	0.448	0.444	0.436	0.407	0.374
40	0.439	0.440	0.438	0.431	0.420	0.392	0.360
45	0.431	0.430	0.426	0.417	0.406	0.377	0.346
50	0.421	0.419	0.413	0.403	0.391	0.362	0.334
60	0.399	0.395	0.387	0.375	0.363	0.337	0.312
−70	0.375	0.369	0.361	0.349			
80	0.351	0.346	0.337	0.325			
90	0.330	0.325					
100	0.311	0.305					
E_p, mv.	−27.7	−25.2	−21.1	−16.4	−11.8	−1.5	+9.8

[a] Potential scale is $(E - E_{1/2})n$.

Table XI. Ratio of Anodic to Cathodic Peak Currents, Case VI

$k_f\tau$	i_a/i_c
0.004	1.00
0.023	0.986
0.035	0.967
0.066	0.937
0.105	0.900
0.195	0.828
0.350	0.727
0.525	0.641
0.550	0.628
0.778	0.551
1.050	0.486
1.168	0.466
1.557	0.415

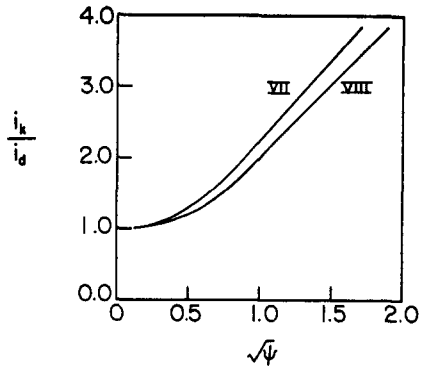

Figure 14. Ratio of kinetic peak current to diffusion controlled peak current

Case VII: $\psi = k_f/a$
Case VIII: $\psi = k_f/b$

the theory of stationary electrode polarography (single sweep method) has been treated by Saveant and Vianello (*39*) who also applied the method in an experimental study (*38*). Since additional correlations can be obtained by considering alternate approaches to the problem, this case will be reviewed briefly. The cyclic triangular wave method has not been treated previously.

Qualitatively, the effect of the chemical reaction on the cathodic portion of the cyclic wave would be an increase in the maximum current. This can be seen by considering the two limiting cases. First, if k_f/a is small, Equation 68 reduces directly to Equation 34, and a reversible stationary electrode polarogram is obtained. At the other limit, for large values of k_f/a, Equation 68 reduces to

$$\chi(at) = \frac{1}{\sqrt{\pi}} \sum_{j=1}^{\infty} (-1)^{j+1} \sqrt{k_f/a} \times \exp\left[-\frac{jnF}{RT}(E - E_{1/2})\right] \quad (83)$$

which indicates that the current is directly proportional to $\sqrt{k_f}$, and independent of the rate of voltage scan, since $\sqrt{a}$ is a coefficient in Equation 25.

Equation 83 can be written in the form

$$i = \frac{nFA\sqrt{Dk_f}\, C_O^*}{1 + \exp\left[\frac{nF}{RT}(E - E_{1/2})\right]} \quad (84)$$

which provides a closed form solution describing the entire wave. Under these conditions, no peak is obtained, and for large values of k_f/a, the potential at which exactly one half of the catalytic limiting current flows is the polarographic $E_{1/2}$. In addition, for very cathodic potentials, Equation 84 reduces to a form derived by Saveant and Vianello (*39*)

$$i = nFAC_O^* \sqrt{Dk_f} \quad (85)$$

which indicates, just as Equation 83, that the limiting current for large values of k_f/a is independent of scan rate.

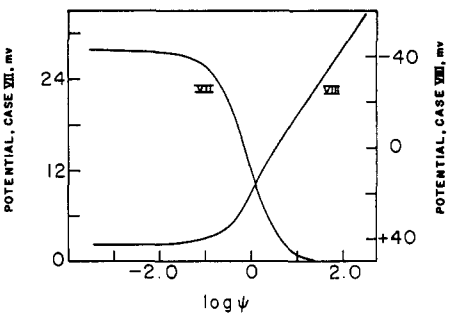

Figure 15. Variation of half-peak potential as a function of kinetic parameters

Case VII: $\psi = k_f/a$; the potential scale is $(E_{p/2} - E_{1/2})n$
Case VIII: $\psi = k_f/b$; the potential scale is $(E_{p/2} - E^\circ)\alpha n_a + (RT/F) \ln \sqrt{\pi Db/k_s}$

Single Scan Method. Since Equation 62 is an Abel integral equation, the solution can be written directly in a manner similar to Case I, Equation 32. This is the approach used by Saveant and Vianello (*39*). Calculations carried out using the numerical method agreed exactly with the results of Saveant and Vianello (for the cathodic portion of the scan) and typical curves are shown in Figure 13. However, the values of $\chi(at)$ presented by Saveant and Vianello do not cover the rising portion and peak of the stationary electrode polarogram at small enough potential intervals to permit convenient calculation of accurate theoretical curves. Thus, additional data are presented in Table XII.

The cathodic current function $\chi(at)$ can be correlated with the kinetic parameter k_f/a by comparison of experimental and theoretical polarograms. However, it is probably more convenient to use a working curve in which the ratio of the catalytic peak current to the reversible peak current is plotted as a function of $(k_f/a)^{1/2}$ (Figure 14). For values of k_f/a larger than about 1.0, the plot is essentially linear, which defines the range of applicability of Equations 84 and 85. For values of k_f/a less than about 0.06, the peak ratio of i_k/i_d is fairly insensitive to changes in k_f/a. The method appears very convenient, but for accurate work with small values of k_f/a a large scale plot of Figure 14 would be required, and the necessary data can be obtained from Tables I and XII.

The variation in peak potential with changes in rate of potential scan also can be used to obtain kinetic data. For low values of k_f/a, the peak potential is

Table XII. Current Functions $\sqrt{\pi}\chi(at)$ for a Catalytic Reaction with Reversible Charge Transfer (Case VII)

Potential[a]	k_f/a 0.04	0.1	0.2	0.4	0.6	1.0	1.78	3.16	10.0
120	0.009	0.010	0.010	0.011	0.012	0.013	0.015	0.019	0.030
100	0.020	0.021	0.021	0.023	0.025	0.028	0.033	0.040	0.066
80	0.042	0.043	0.045	0.049	0.052	0.059	0.069	0.086	0.139
60	0.086	0.088	0.093	0.100	0.108	0.121	0.144	0.176	0.289
50	0.120	0.123	0.129	0.140	0.150	0.170	0.201	0.249	0.409
45	0.140	0.145	0.152	0.165	0.178	0.201	0.239	0.294	0.482
40	0.163	0.168	0.177	0.193	0.207	0.234	0.279	0.345	0.567
35	0.189	0.195	0.205	0.224	0.242	0.273	0.326	0.403	0.665
30	0.216	0.224	0.236	0.258	0.278	0.315	0.378	0.467	0.773
25	0.245	0.254	0.267	0.294	0.318	0.361	0.433	0.539	0.894
20	0.275	0.285	0.301	0.331	0.359	0.409	0.493	0.614	1.022
15	0.306	0.318	0.337	0.371	0.403	0.461	0.558	0.695	1.162
10	0.336	0.349	0.370	0.410	0.447	0.512	0.623	0.782	1.310
5	0.364	0.380	0.404	0.449	0.491	0.566	0.690	0.867	1.459
0	0.391	0.408	0.436	0.487	0.534	0.617	0.756	0.955	1.614
−5	0.414	0.434	0.465	0.522	0.574	0.668	0.821	1.042	1.769
10	0.432	0.455	0.489	0.552	0.611	0.715	0.883	1.124	1.919
15	0.448	0.472	0.510	0.580	0.644	0.757	0.942	1.204	2.061
20	0.459	0.485	0.527	0.604	0.673	0.796	0.996	1.278	2.197
25	0.465	0.494	0.540	0.622	0.697	0.829	1.044	1.345	2.322
−30	0.468	0.499	0.548	0.638	0.719	0.861	1.088	1.406	2.436
35	0.467	0.500	0.553	0.649	0.735	0.885	1.126	1.462	2.540
40	0.463	0.499	0.556	0.658	0.749	0.907	1.159	1.510	2.633
45	0.457	0.495	0.555	0.663	0.759	0.924	1.188	1.552	2.713
50	0.450	0.490	0.553	0.666	0.766	0.939	1.211	1.587	2.782
−60	0.431	0.476	0.545	0.668	0.776	0.961	1.250	1.644	2.894
80	0.390	0.442	0.522	0.662	0.782	0.984	1.295	1.715	3.034
100	0.354	0.413	0.502	0.653	0.781	0.994	1.315	1.749	3.102
120	0.326	0.390	0.486	0.646	0.779	0.997	1.326	1.765	3.134
140	0.305	0.374	0.474	0.641	0.777	0.999	1.330	1.772	3.149
$E_{p/2}$, mv.	+27.3	25.7	23.5	19.6	16.3	11.2	6.7	3.8	1.0

[a] Potential scale is $(E - E_{1/2})n$.

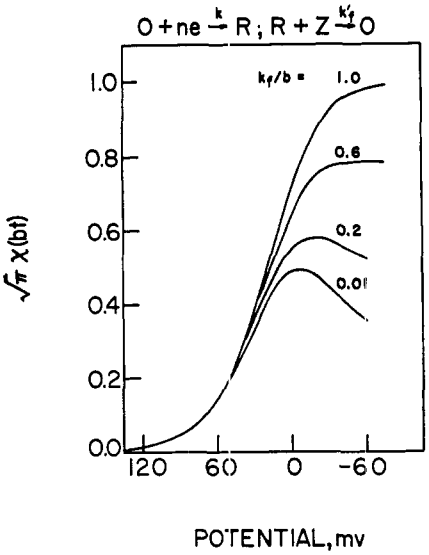

Figure 16. Stationary electrode polarograms, Case VIII

Potential scale is $(E - E^\circ)\alpha n_a + (RT/F) \ln \sqrt{\pi Db}/k_s$

independent of k_f/a, and is constant at $28.5/n$ mv. cathodic of $E_{1/2}$ as in the reversible case. As k_f/a increases, the peak potential shifts cathodically by about $60/n$ mv. for a ten-fold increase in k_f/a but simultaneously, the peak becomes quite broad, and for values of k_f/a larger than about 1.0, no peak is observed. Thus, it is more useful to correlate half-peak potentials with k_f/a [as suggested by Saveant (*38*)] since this correlation can be extended to the region where no peak is observed. As predicted from Equation 84, when k_f/a is larger than about 10, the potential at which the current is equal to half of the limiting current is independent of variations of k_f/a, and is equal to the polarographic half-wave potential. The behavior for intermediate values of k_f/a is shown in Figure 15, and the data for an accurate plot can be obtained from Table XII.

Spherical Electrodes. For the catalytic case, Weber (*51*) was able to derive a spherical correction term in closed form, which is the same as the one derived by Reinmuth for the reversible case (*35*). Thus, the value of $\phi(at)$ listed in Table I can be used directly with the values of $\chi(at)$ in Table XII to calculate the current at a spherical electrode.

Cyclic Triangular Wave Method. Provided a switching potential is selected at least $35/n$ mv. cathodic of the peak potential, the anodic curve (as measured to the extension of the cathodic curve) is the same shape as the cathodic curve, independent of both the switching potential and k_f/a. The ratio of the cathodic peak current to the anodic peak current is unity, exactly as in the reversible case. At large values of k_f/a—e.g., larger than about 1.0—where no cathodic peak is observed, anodic peaks are not observed either, and on the anodic scan, the current simply returns to zero at potentials corresponding to the foot of the cathodic wave.

Since the anodic portion of the scan has exactly the same properties as the cathodic, no additional quantitative kinetic information can be obtained.

VIII. CATALYTIC REACTION WITH IRREVERSIBLE CHARGE TRANSFER

For catalytic systems in which both the charge transfer reaction and the chemical reaction are irreversible,

$$O + ne \xrightarrow{k} R \qquad R + Z \xrightarrow{k'_f} O \qquad \text{(VIII)}$$

the theory of stationary electrode polarography has not been considered previously. Qualitatively, one would expect that the polarograms would be similar to the catalytic case with reversible charge transfer, except that the curves would be lower and more spread out on the potential axis. In addition, no anodic current would be

Table XIII. Current Functions $\sqrt{\pi}\chi(bt)$ for a Catalytic Reaction with Irreversible Charge Transfer (Case VIII)

	k_f/b								
Potential[a]	0.04	0.1	0.2	0.4	0.6	1.0	1.78	3.16	10.0
160	0.004	0.004	0.004	0.004	0.004	0.004	0.004	0.004	0.004
140	0.008	0.008	0.008	0.008	0.008	0.008	0.008	0.008	0.008
120	0.016	0.016	0.016	0.016	0.016	0.016	0.016	0.016	0.016
110	0.024	0.024	0.024	0.024	0.024	0.024	0.024	0.024	0.024
100	0.035	0.035	0.035	0.035	0.035	0.035	0.035	0.036	0.036
90	0.050	0.050	0.051	0.051	0.051	0.051	0.051	0.052	0.052
80	0.072	0.073	0.073	0.073	0.074	0.074	0.075	0.075	0.076
70	0.104	0.105	0.105	0.106	0.107	0.108	0.109	0.110	0.113
60	0.145	0.147	0.147	0.148	0.150	0.152	0.155	0.157	0.162
50	0.198	0.200	0.201	0.205	0.208	0.213	0.218	0.224	0.234
40	0.264	0.267	0.271	0.278	0.283	0.291	0.302	0.313	0.334
35	0.301	0.305	0.311	0.320	0.327	0.339	0.354	0.370	0.399
30	0.334	0.344	0.349	0.362	0.372	0.388	0.409	0.430	0.471
25	0.376	0.383	0.392	0.408	0.422	0.444	0.473	0.500	0.558
20	0.410	0.418	0.431	0.453	0.470	0.498	0.534	0.574	0.650
15	0.443	0.454	0.470	0.500	0.521	0.556	0.600	0.656	0.761
10	0.469	0.483	0.503	0.538	0.567	0.612	0.673	0.740	0.876
5	0.490	0.506	0.532	0.575	0.610	0.666	0.742	0.827	1.002
0	0.504	0.524	0.555	0.608	0.651	0.719	0.813	0.920	1.145
−5	0.511	0.534	0.571	0.633	0.685	0.766	0.878	1.007	1.288
−10	0.511	0.539	0.581	0.653	0.713	0.809	0.941	1.097	1.443
15	0.506	0.538	0.586	0.667	0.735	0.844	0.998	1.178	1.595
20	0.497	0.532	0.585	0.676	0.753	0.875	1.049	1.258	1.755
25	0.485	0.523	0.581	0.681	0.765	0.900	1.094	1.328	1.903
30	0.470	0.512	0.575	0.683	0.774	0.921	1.133	1.394	2.053
−35	0.456	0.500	0.568	0.683	0.780	0.937	1.166	1.450	2.186
40	0.440	0.487	0.559	0.681	0.783	0.951	1.195	1.502	2.317
50	0.411	0.463	0.541	0.674	0.786	0.969	1.238	1.583	2.538
60	0.386	0.442	0.525	0.667	0.786	0.980	1.269	1.643	2.710
70	0.366	0.425	0.512	0.661	0.785	0.988	1.289	1.684	2.840
−80	0.348	0.409	0.501	0.655	0.783	0.992	1.303	1.714	2.936
100	0.320	0.386	0.484	0.646	0.780	0.997	1.320	1.748	3.056
120	0.300	0.371	0.473	0.641	0.778	0.999	1.328	1.764	3.112
140			0.466	0.638	0.776	0.999	1.331	1.772	3.139
160			0.461	0.636	0.776	1.000	1.332	1.776	3.152
$E_{p/2}$, mv.	+41.1	39.6	37.0	32.4	27.7	19.8	10.3	1.3	−14.4

[a] Potential scale is $(E - E^\circ)\,\alpha n_a + (RT/F) \ln \sqrt{\pi Db}/k_s$.

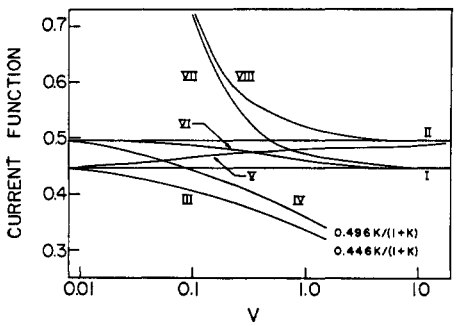

Figure 17. Variation of peak current functions with rate of voltage scan

observed in a cyclic triangular wave experiment.

Again, two limiting cases can be considered. For small values of k_f/b, Equation 69 reduces to Equation 48 and an irreversible stationary electrode polarogram is obtained. For large values of k_f/b, Equation 69 reduces to

$$\chi(bt) = \frac{1}{\sqrt{\pi}} \sum_{j=1}^{\infty} (-1)^{j+1} (\sqrt{\pi})^j \sqrt{k_f/b} \times \exp\left[-\frac{j\alpha n_a F}{RT} \left(E - E^\circ + \frac{RT}{\alpha n_a F} \times \ln \frac{\sqrt{\pi D b}}{k_s} + \frac{RT}{\alpha n_a F} \ln \sqrt{\frac{k_f}{\pi a}} \right) \right] \quad (86)$$

and analogous to Case VII under these conditions, the current is directly proportional to $\sqrt{k_f}$, and is independent of b.

Similarly, a closed form solution describing the entire wave can be obtained by rearranging Equation 86

$$i = \frac{nFAC_o^* \sqrt{Dl_f}}{1 + \exp\left[\frac{\alpha n_a F}{RT} \left(E - E^\circ + \frac{RT}{\alpha n_a F} \ln \frac{\sqrt{\pi D b}}{k_s} + \frac{RT}{\alpha n_a F} \ln \sqrt{\frac{k_s}{\pi a}} \right) \right]} \quad (87)$$

Typical curves for several values of k_f/b are shown in Figure 16 and the data are listed in Table XIII. These curves qualitatively are similar to those of Figure 14 except that $\chi(bt)$, k_f/b and the potential axis all depend on αn_a.

For quantitative characterization of the kinetics, the data can be treated in a manner similar to the catalytic reaction coupled to a reversible charge transfer. In this case, however, the ratio of the catalytic current to the irreversible current for the system is the parameter used. The working curve for this case is included in Figure 14. As in the previous case, the ratio i_k/i_d is fairly insensitive to changes in k_f/b less than about 0.06, and the points required for a large scale plot of the working curve can be obtained from Tables III and XIII.

The variation of the half-peak potential with changes in k_f/b also can be used to characterize the system. A working curve for this method is shown in Figure 15, and the data can be obtained from Table XIII.

DIAGNOSTIC CRITERIA

In each of the kinetic cases, the effect of the chemical reaction will depend on its rate, as compared with the time required to perform the experiment. Taking Case V (irreversible succeeding chemical reaction) as an example, if a very rapid reaction is involved in experiments with very slow scan rates, the stationary electrode polarogram will reflect the characteristics of the chemical step almost entirely. On the other hand, if the rate of voltage scan is rapid compared to the rate of the reaction, the curves are identical to those for the corresponding uncomplicated charge transfer.

Similar observations can be extended to the other kinetic cases, and are borne out quantitatively in the theory presented here—i.e., in every kinetic case, the ratio of the rate constant to the rate of voltage scan appears in the kinetic parameter. This, in turn, makes it possible to use these relations to define diagnostic criteria for the investigation of unknown systems.

Although there are innumerable correlations which could be made, perhaps those which are most useful experimentally are the variation—with changes in rate of voltage scan—of the cathodic peak current, the cathodic peak (or half-peak) potential, and the ratio of the anodic to cathodic peak currents. These diagnostic relations are most useful for qualitative characterization of unknown systems, since only trends in the experimental behavior are required. Therefore, the correlations in Figures 17, 18 and 19, have all been calculated for an arbitrary value of rate constant (and equilibrium constant, if necessary) so that the behavior could be compared readily on the same diagram.

Among the relations to be noted in Figure 17 is that by plotting the quantity $i_p/nFA\sqrt{Da}\,C_o^*$ as a function of the rate of voltage scan, the effect of

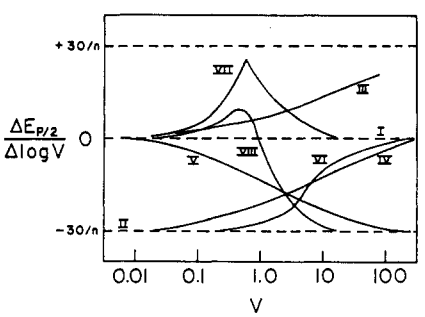

Figure 18. Rate of shift of potential as a function of scan rate

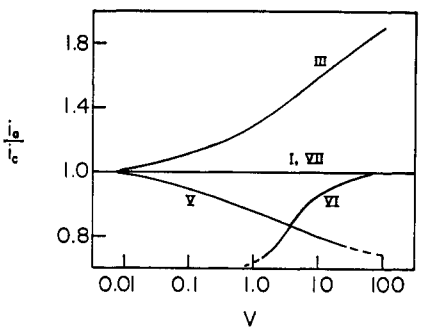

Figure 19. Ratio of anodic to cathodic peak currents as a function of rate of voltage scan

v on the diffusion process can be separated from its effect on the kinetics. Thus, for the uncomplicated charge transfer reactions (Cases I and II) horizontal straight lines are obtained. The behavior for each kinetic case approaches one of these straight lines when the rate of voltage scan is such that the chemical reaction cannot proceed significantly before the experiment is over. Experimentally, this correlation is extremely easy to obtain, since it is only necessary to plot $i_p/v^{1/2}$ *vs.* v.

The rate at which the wave shifts along the potential axis as the rate of voltage scan is varied (Figure 18) is also useful for investigation of unknown systems. Because several of the cases do not exhibit peaks under some conditions, the half-peak potential was used in this correlation. However, these curves apply as well to the peak potential for Cases I, II, V, and VI.

In Figure 19, which is relevant only for reversible charge transfers, the ratio of anodic peak current to the cathodic peak current is unity for the reversible (Case I) and catalytic (Case VII) systems only, and this serves as a quick test for the presence of kinetic complications.

In some of the individual cases, additional experimental correlations are particularly useful. For example, if an irreversible charge transfer reaction is involved, it is always possible to obtain αn_a from the shift in peak potential, provided the rate of voltage scan is in the proper range. For reversible charge transfer, other correlations are possible involving variation in anodic peak current or peak potential with switching potential. However, these correlations can be defined more easily in connection with experimental results on a particular kinetic case. Several studies involving applications of the theory presented here are now in progress, and these, with the additional correlations, will be presented in the future.

Although various electrochemical methods have been developed recently which can be used for similar measurements on kinetic systems, stationary electrode polarography appears to be

particularly convenient to use. From the experimental point of view, the time scale of the experiment can be varied from conventional polarographic rates of voltage scan of a few millivolts per second (where convection ultimately sets the lower limit of scan rate) to perhaps several thousand volts per second (where charging current and adsorption phenomena become important). Furthermore, this extremely wide range of scan rates can be obtained with ease if instruments based on operational amplifiers are available (*42, 49*). Thus, the use of the diagnostic criteria is particularly simple, and stationary electrode polarography is a very powerful method for studying electrochemical kinetics.

ACKNOWLEDGMENT

The numerical calculations were carried out at the Midwest Universities Research Association and the help of M. R. Storm in making available the IBM 704 computer is gratefully acknowledged. During the academic year 1962-63, R. S. Nicholson held the Dow Chemical Fellowship at the University of Wisconsin.

LITERATURE CITED

(1) Apostol, T. M., "Mathematical Analysis," p. 200, Addison Wesley, Reading, Mass., 1957.
(2) Berzins, T., Delahay, P., *J. Am. Chem. Soc.* **75,** 555 (1953).
(3) Buck, R. P., ANAL. CHEM. **36,** 947 (1964).
(4) Delahay, P., *J. Am. Chem. Soc.* **75,** 1190 (1953).
(5) Delahay, P., "New Instrumental Methods in Electrochemistry," Ch. 3, Interscience, New York, 1954.
(6) *Ibid.*, Chap. 6.
(7) DeMars, R. D., Shain, I., ANAL. CHEM. **29,** 1825 (1957).
(8) DeMars, R. D., Shain, I., *J. Am. Chem. Soc.* **81,** 2654 (1959).
(9) Frankenthal, R. P., Shain, I., *Ibid.*, **78,** 2969 (1956).
(10) Galus, Z., Adams, R. N., *J. Phys. Chem.* **67,** 862 (1963).
(11) Galus, Z., Lee, H. Y., Adams, R. N., *J. Electroanal. Chem.* **5,** 17 (1963).
(12) Gokhshtein, A. Y., Gokhshtein, Y. P., *Doklady Akad. Nauk SSSR* **131,** 601 (1960).
(13) Gokhshtein, Y. P., *Ibid.*, **126,** 598 (1959).
(14) Gokhshtein, Y. P., Gokhshtein, A. Y., in "Advances in Polarography," I. S. Longmuir, ed., **Vol. II,** p. 465, Pergamon Press, New York, 1960.
(15) Gokhshtein, Y. P., Gokhshtein, A. Y., *Doklady Akad Nauk SSSR* **128,** 985 (1959).
(16) Kemula, W., in "Advances in Polarography," I. S. Longmuir, ed., **Vol. I,** p. 105, Pergamon Press, New York, 1960.
(17) Kemula, W., Kublik, Z., *Anal. Chim. Acta* **18,** 104 (1958).
(18) Kemula, W., Kublik, Z., *Bull. Acad. Polon. Sci., Ser. Sci. Chim., Geol. et Geograph.* **6,** 661 (1958).
(19) Koutecky, J., *Collection Czechoslov. Chem. Communs.* **21,** 433 (1956).
(20) Koutecky, J., Brdicka, R., *Ibid.*, **12,** 337 (1947).
(21) Matheson, L. A., Nichols, N., *Trans. Electrochem. Soc.* **73,** 193 (1938).
(22) Matsuda, H., *Z. Elektrochem.* **61,** 489 (1957).
(23) Matsuda, H., Ayabe, Y., *Ibid.*, **59,** 494 (1955).
(24) Mueller, T. R., Adams, R. N., *Anal. Chim. Acta* **25,** 482 (1961).
(25) Nicholson, M. M., *J. Am. Chem. Soc.* **76,** 2539 (1954).
(26) Nicholson, M. M., *Ibid.*, **79,** 7 (1957).
(27) Nicholson, R. S., Ph.D. Thesis, University of Wisconsin, 1964.
(28) Papoff, P., *J. Am. Chem. Soc.* **81,** 3254 (1959).
(29) Randles, J. E. B., *Trans. Faraday Soc.* **44,** 327 (1948).
(30) Reinmuth, W. H., ANAL. CHEM. **32,** 1891 (1960).
(31) Reinmuth, W. H., *Ibid.*, **33,** 185 (1961).
(32) *Ibid.*, p. 1793.
(33) Reinmuth, W. H., *Ibid.*, **34,** 1446 (1962).
(34) Reinmuth, W. H., Columbia University, New York, N. Y., unpublished data, 1964.
(35) Reinmuth, W. H., *J. Am. Chem. Soc.* **79,** 6358 (1957).
(36) Riha, J. in "Progress in Polarography," P. Zuman, ed., **Vol. II,** Chap. 17, Interscience, New York, 1962.
(37) Ross, J. W., DeMars, R. D., Shain, I., ANAL. CHEM. **28,** 1768 (1956).
(38) Saveant, J. M., Ecole Normale Superieure, Paris, private communication, 1963.
(39) Saveant, J. M., Vianello, E., in "Advances in Polarography," I. S. Longmuir, ed., **Vol. I,** p. 367, Pergamon Press, New York, 1960.
(40) Saveant, J. M., Vianello, E., *Compt. Rend.* **256,** 2597 (1963).
(41) Saveant, J. M., Vianello, E., *Electrochim. Acta* **8,** 905 (1963).
(42) Schwarz, W. M., Shain, I., ANAL. CHEM. **35,** 1770 (1963).
(43) Schwarz, W. M., Shain, I., Division of Physical Chemistry, 142nd National Meeting, ACS Atlantic City, N. J., September 1962.
(44) Sevcik, A., *Collection Czechoslov. Chem. Communs.* **13,** 349 (1948).
(45) Shain, I., in "Treatise on Analytical Chemistry," Kolthoff and Elving, eds., **Part I,** Sec. D-2, Chap. 50, Interscience, New York, 1963.
(46) Shain, I., Southeast Regional Meeting, ACS, New Orleans, December 1961.
(47) Smutek, M., *Collection Czechoslov. Chem. Communs.* **20,** 247 (1955).
(48) Tricomi, F. G., "Integral Equations," p. 39, Interscience, New York, 1957.
(49) Underkofler, W. L., Shain, I., ANAL. CHEM. **35,** 1778 (1963).
(50) Vogel, J., in "Progress in Polarography," P. Zuman, ed., **Vol. II,** Chap. 20, Interscience, New York, 1962.
(51) Weber, J., *Collection Czechoslov. Chem. Communs.* **24,** 1770 (1959).

RECEIVED for review November 5, 1963. Accepted December 30, 1963. This work was supported in part by funds received from the U. S. Atomic Energy Commission under Contract No. AT(11-1)-1083. Other support was received from the National Science Foundation under Grant No. G15741.

New Electrodes for Chronopotentiometry in Thin Layers of Solution

A. T. HUBBARD and FRED C. ANSON

California Institute of Technology, Pasadena, Calif.

▶ **Two new electrodes for chronopotentiometry in thin layers of solution are introduced and the details of their construction and manipulation are presented. In addition to giving more reproducible results, these electrodes are more convenient to use than previous designs. A typical set of data is presented, demonstrating the reproducibility of the experimental transition times and their agreement with transition times calculated with Faraday's law from the simple geometrical volume of the electrode crevices.**

IN PREVIOUS STUDIES (*2, 3*) the theory of thin layer chronopotentiometry was presented and tested with a specially constructed electrode for which the dimensions of the solution reservoir were somewhat smaller than those of the diffusion layer. This electrode suffered from the fact that it had to be filled under reduced pressure and several hours were needed to wash out the electrode cavity after each use.

In the present work two new electrodes have been devised that are simple to construct and may be rapidly filled and cleaned. The first electrode imprisons the thin layer of solution between the inner wall of a short section of precision-bore glass capillary tubing and a close-fitting platinum wire inserted into the tubing (Figure 1). The second electrode is constructed from a micrometer to which platinum faces have been attached; a thin layer of solution is confined between the faces of the micrometer which are equipotential (Figure 2).

These electrodes are quite convenient to use, and yield more reproducible re-